Semiconductor magnetooptics

various ways of seeing spins

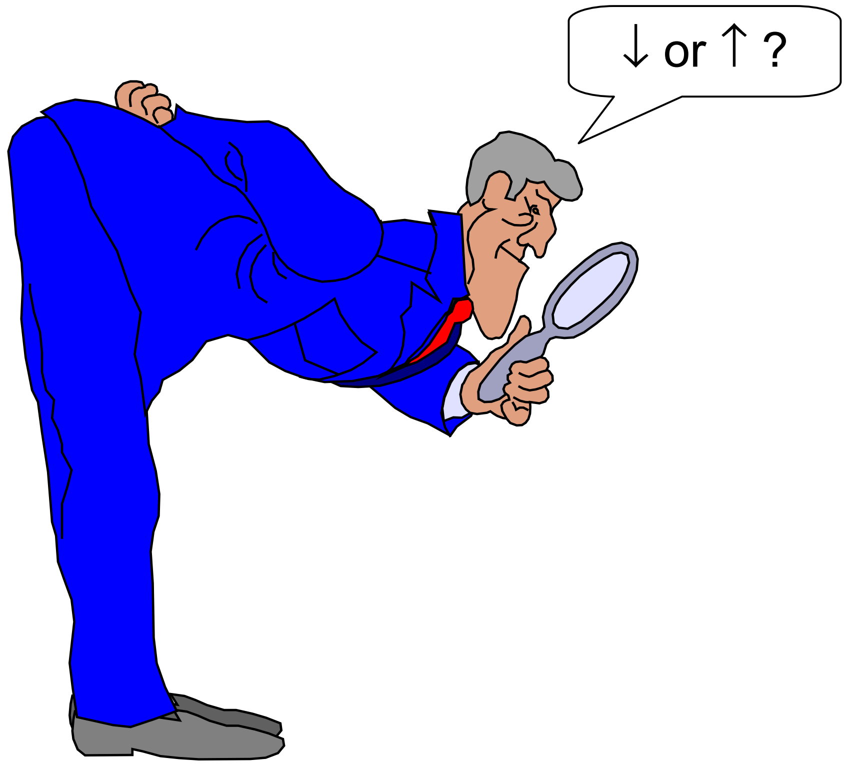

Jan Gaj gaj@fuw.edu.pl;

Physics Department, Warsaw University

August 1-5, 2005 Spintech III, Awaji Island, Japan

Outline

- Where? What?
- Fundamentals
  - Faraday and Kerr rotation
  - Magnetic circular dichroism
  - PL polarization,
- Seeing spins in experiments
  - spin energy: Zeeman effect in absorption, Faraday and Kerr rotation
  - average spin - magnetization (also spontaneous) : PL polarization
  - efficiency of spin injection: PL
  - carrier spin polarization: Faraday
  - magnetic ion spin temperature: PL
  - electron spin dynamics: time-resolved Kerr
  - spatial distribution: spin mapping: PL, Kerr

Where?

- Medium and large gap semiconductors
- Interband transitions
- Bulk crystals and quantum wells

What?

- Information about spins of carriers, excitons, magnetic ions

Fundamentals

Faraday, Kerr, MCD, PL

Faraday configuration

- In an isotropic medium all the polarizations represent eigenmodes of the electromagnetic wave.

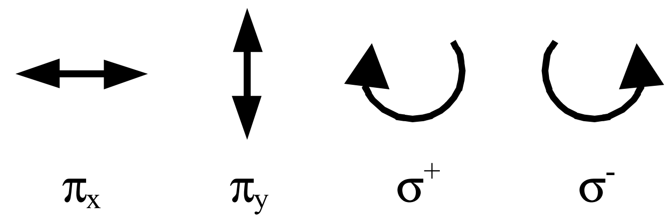

- in Faraday configuration only σ^+ and σ^- represent eigenmodes.

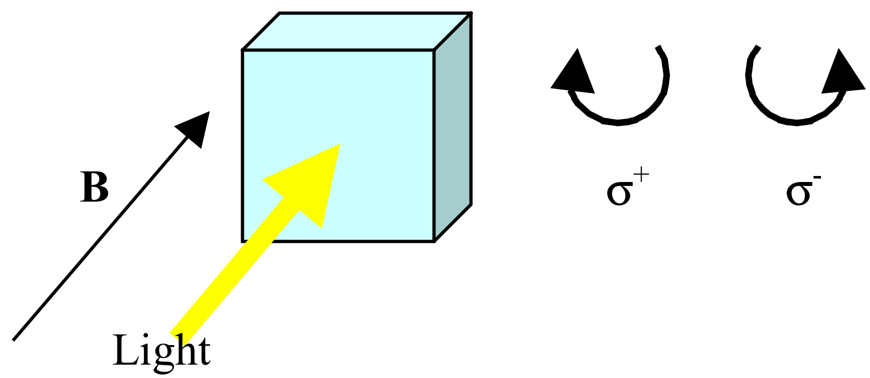

- polarization-dependent complex refraction index

$$\tilde{n}_\pm = n_\pm - i\kappa_\pm$$

Dispersion relations

- Origin: causality principle
- Detailed form: symmetry of the response function
- Without magnetic field: Kramers – Kronig form

$$n(\omega)-1=-\frac{2}{\pi}\int_0^\infty \frac{\omega'\kappa(\omega')d\omega'}{\omega^2-\omega'^2} \qquad \kappa(\omega)=\frac{2\omega}{\pi}\int_0^\infty \frac{(n(\omega')-1)d\omega'}{\omega^2-\omega'^2}$$

- Applying DR to the experimental data: difficult
- Hint: modeling with real and imaginary part of a complex function (e.g., Lorentzian)

See, e.g., F. Byron and R. Fuller, *Mathematics of Classical and Quantum Physics* (Addison-Wesley, Reading, MA, 1969).

Faraday rotation

- Decomposition of linearly polarized light in two circularly polarized waves

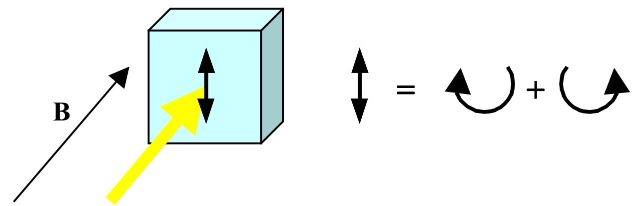

- Phase shift

$$\delta = \frac{\omega}{c}\left(n_{+} - n_{-}\right)d$$

- Rotation
  of the polarization plane

$$\vartheta = \tfrac{1}{2}\delta = \frac{\omega}{2c}\left(n_{+} - n_{-}\right)d$$

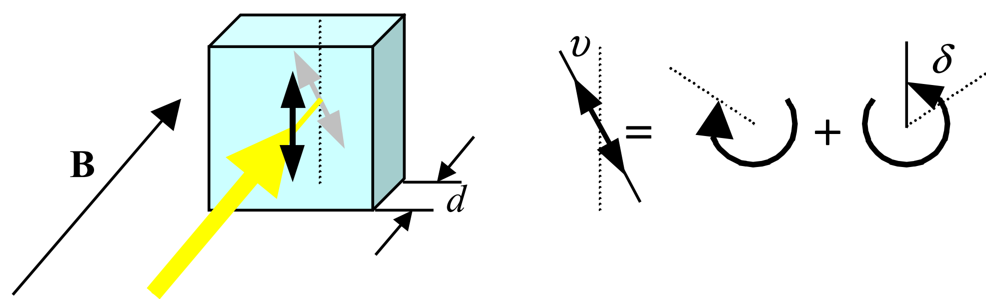

Example: modeling Faraday rotation of a single absorption line

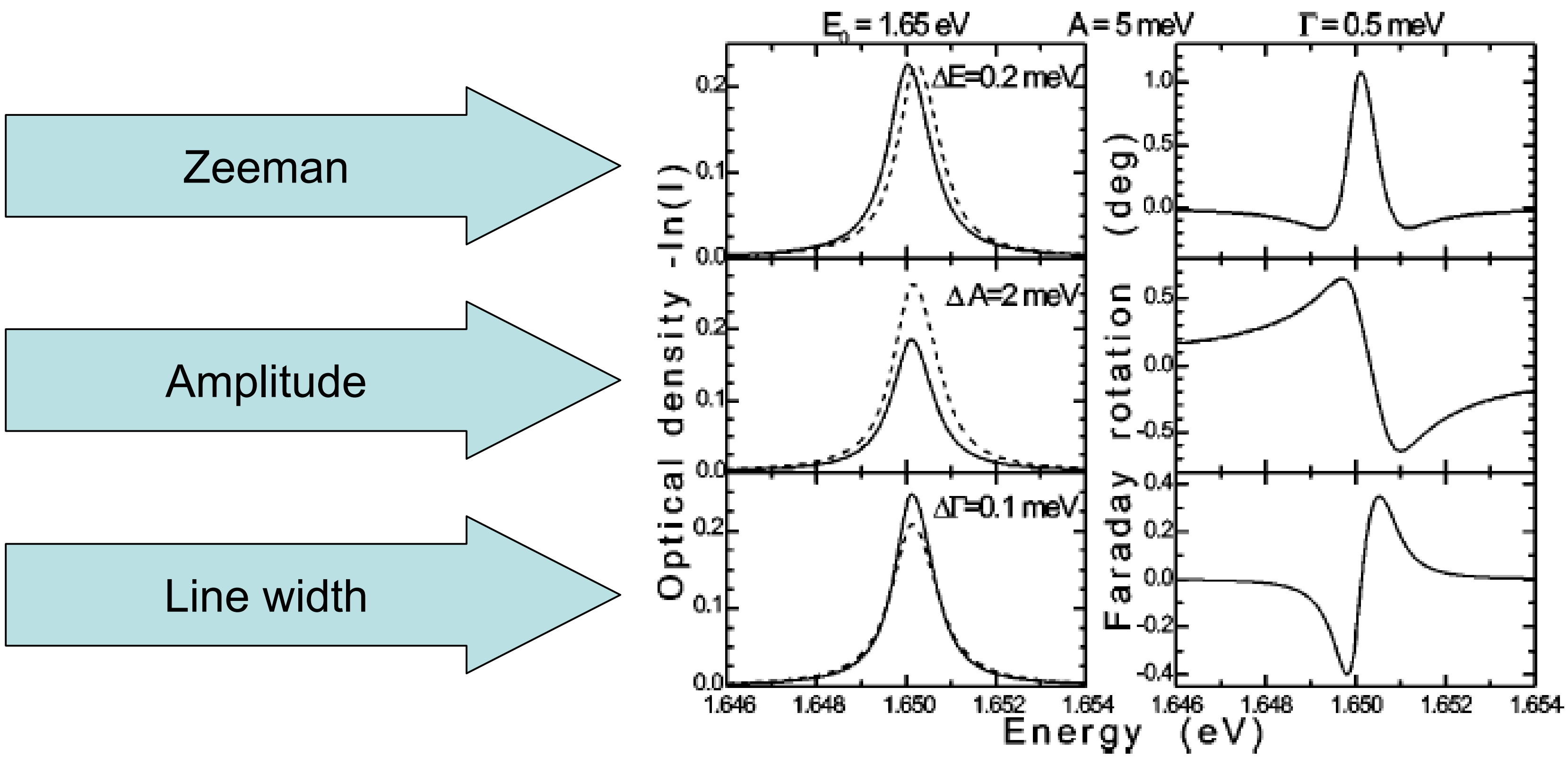

$$t = |t|e^{i\varphi} = \sqrt{T}e^{i\varphi} \qquad 2\ln t = \ln T + 2i\varphi$$

W. Maślana et al., Phys. Rev. B **63,** 165318 (2001)

Kerr rotation

- Phase shift between the two circularly polarized components on reflection
- Cause: magnetic field or magnetization.
- Simplest case: Faraday geometry (polar Kerr effect).

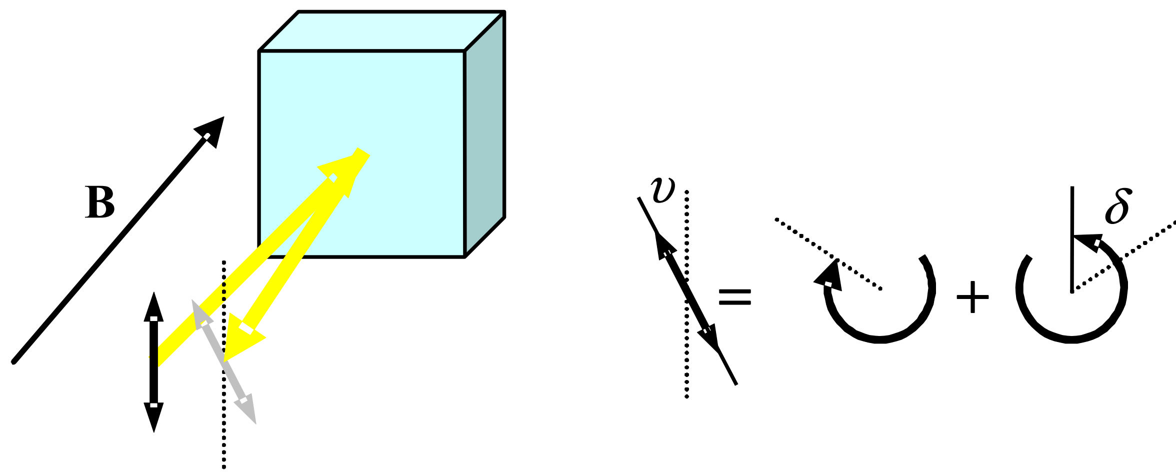

Kerr rotation

Backscattering geometry

Amplitude (r) and intensity (R) reflection coefficients

$$r = \frac{\tilde{n}-1}{\tilde{n}+1} = \frac{n-1-i\kappa}{n+1-i\kappa} = |r|e^{i\varphi} = \sqrt{R}e^{i\varphi} \qquad R = \frac{(n-1)^2+\kappa^2}{(n+1)^2+\kappa^2}$$

Kerr rotation angle

$$\vartheta_K = \tfrac{1}{2}\delta_K = \tfrac{1}{2}\left(\varphi_+ - \varphi_-\right)$$

$$2\ln r = \ln R + 2i\varphi$$

Dispersion relations between $\ln R$ and 2φ useful for modeling

Magnetic Circular Dichroism

difference in intensity

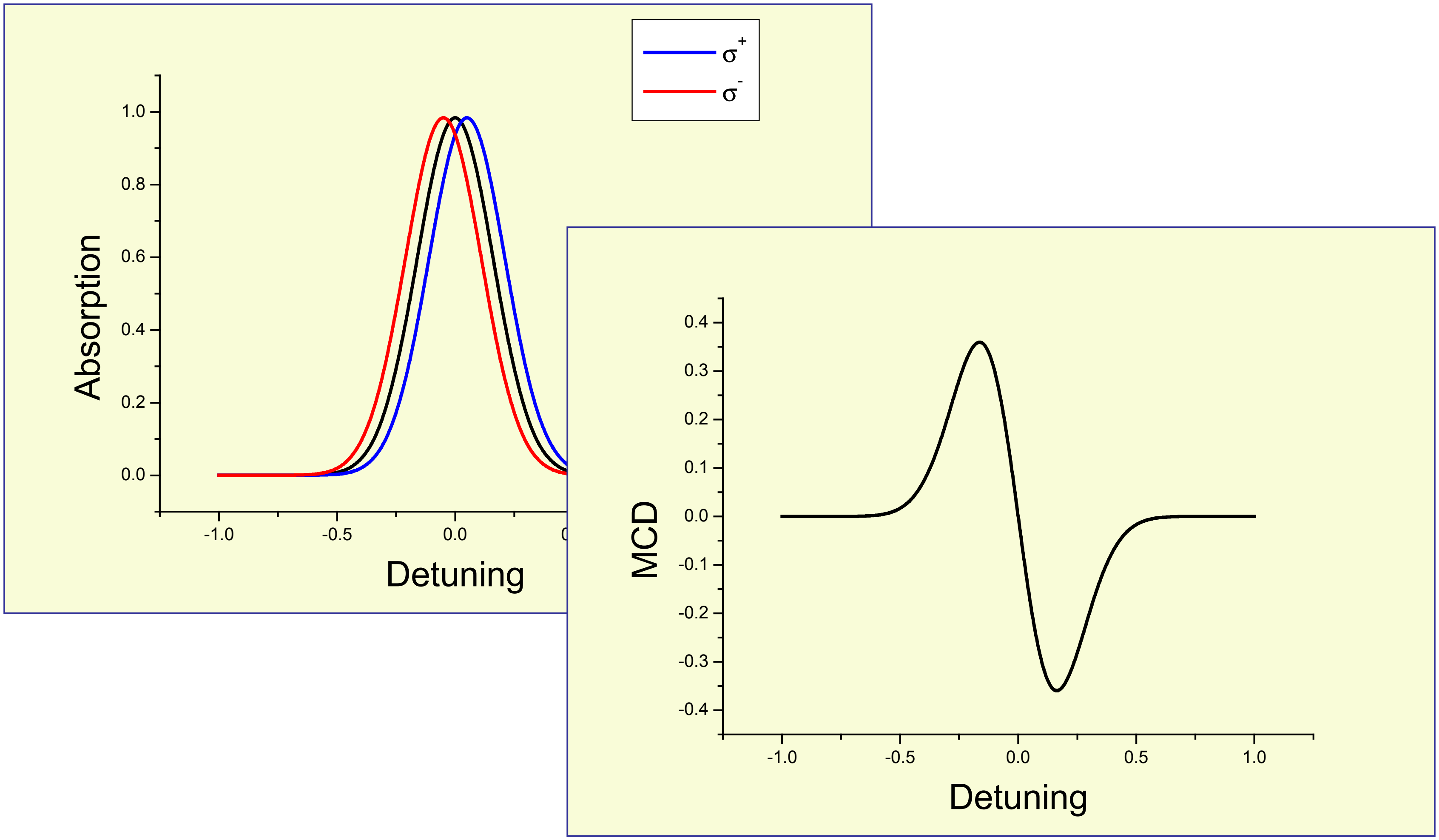

Real and effective magnetic field

- Magnetic field influences carriers.

$$H = H_o + H_s; \quad H_s = g\mu_B \mathbf{B}\cdot\boldsymbol{\sigma}$$

- Interaction with magnetic ions:

$$H_{exch} = \sum_j J(\mathbf{r}-\mathbf{R_j})\mathbf{S_j}\cdot\boldsymbol{\sigma}$$

- The effective (exchange) field acts only on the carrier spin!

$$\mathbf{B}_{eff} = \frac{1}{g\mu_B}\sum_j J(\mathbf{r}-\mathbf{R_j})\mathbf{S_j}$$

- Proportionality to magnetization

- In most cases:

$$H_{exch} >> H_s, H_o$$

See, e.g., J.K. Furdyna, J. Appl. Phys. 64, R29 (1988)

Diluted magnetic semiconductor

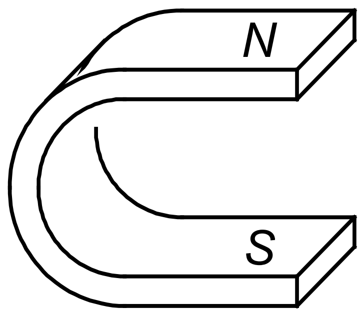

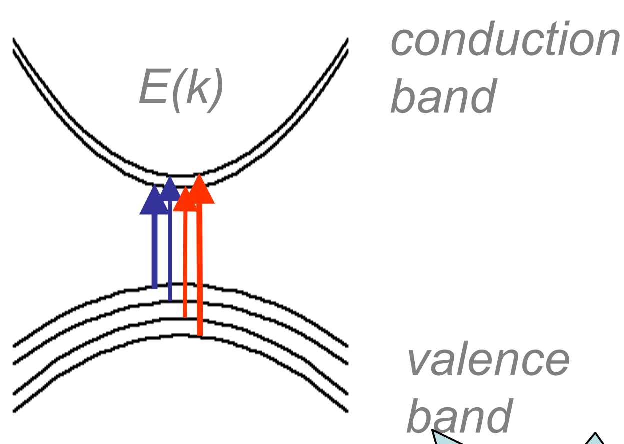

approximation: wavevector in presence of magnetic field!

Bulk (zincblende)

- *excitonic absorption spectrum*

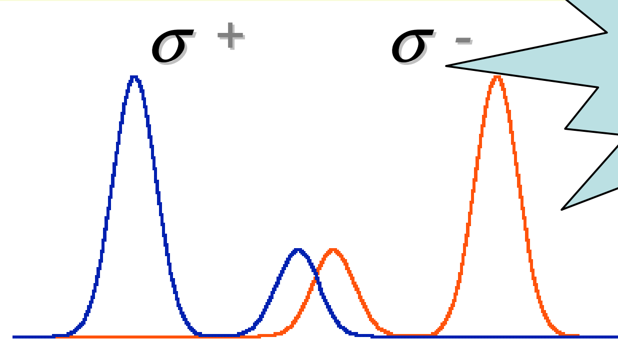

effective field proportional to magnetization (mean field approximation)

$$H = N_0 \alpha x \langle \mathbf{S} \rangle \cdot \boldsymbol{\sigma}_c \qquad H = N_0 \beta\, x \langle \mathbf{S} \rangle \cdot \boldsymbol{\sigma}_v$$

Diluted magnetic semiconductor

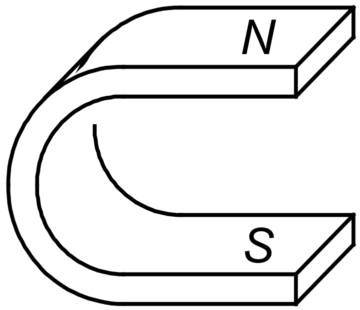

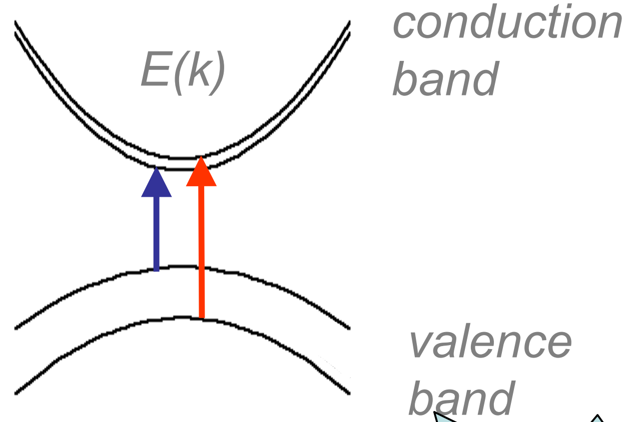

approximation: wavevector in presence of magnetic field!

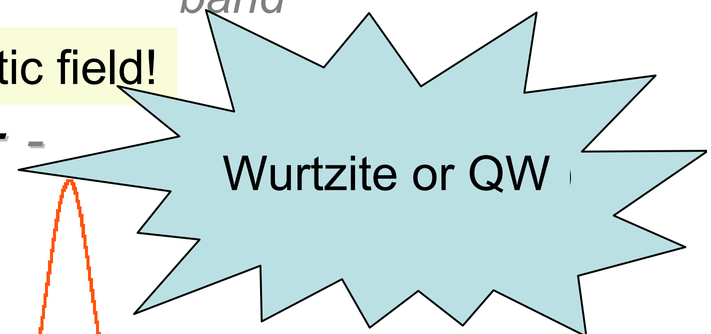

- *excitonic absorption spectrum*

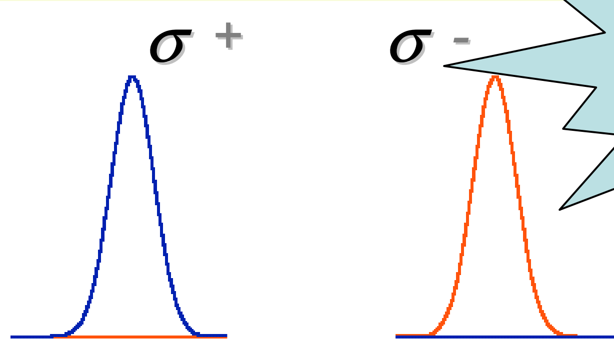

effective field proportional to magnetization (mean field approximation)

$$H = N_0 \alpha x \langle \mathbf{S} \rangle \cdot \boldsymbol{\sigma}_c \qquad H = N_0 \beta x \langle \mathbf{S} \rangle \cdot \boldsymbol{\sigma}_v$$

Photoluminescence polarization

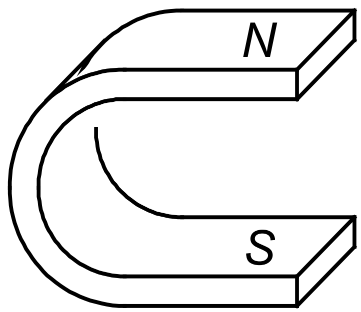

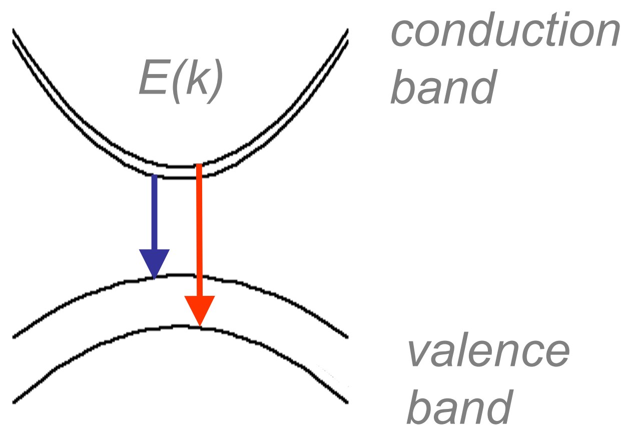

- *PL spectrum*

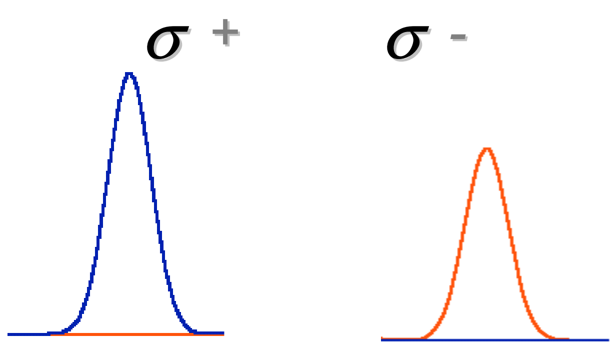

$$I_+/I_- = N_\uparrow/N_\downarrow$$

valid also without magnetic field!

Various configurations

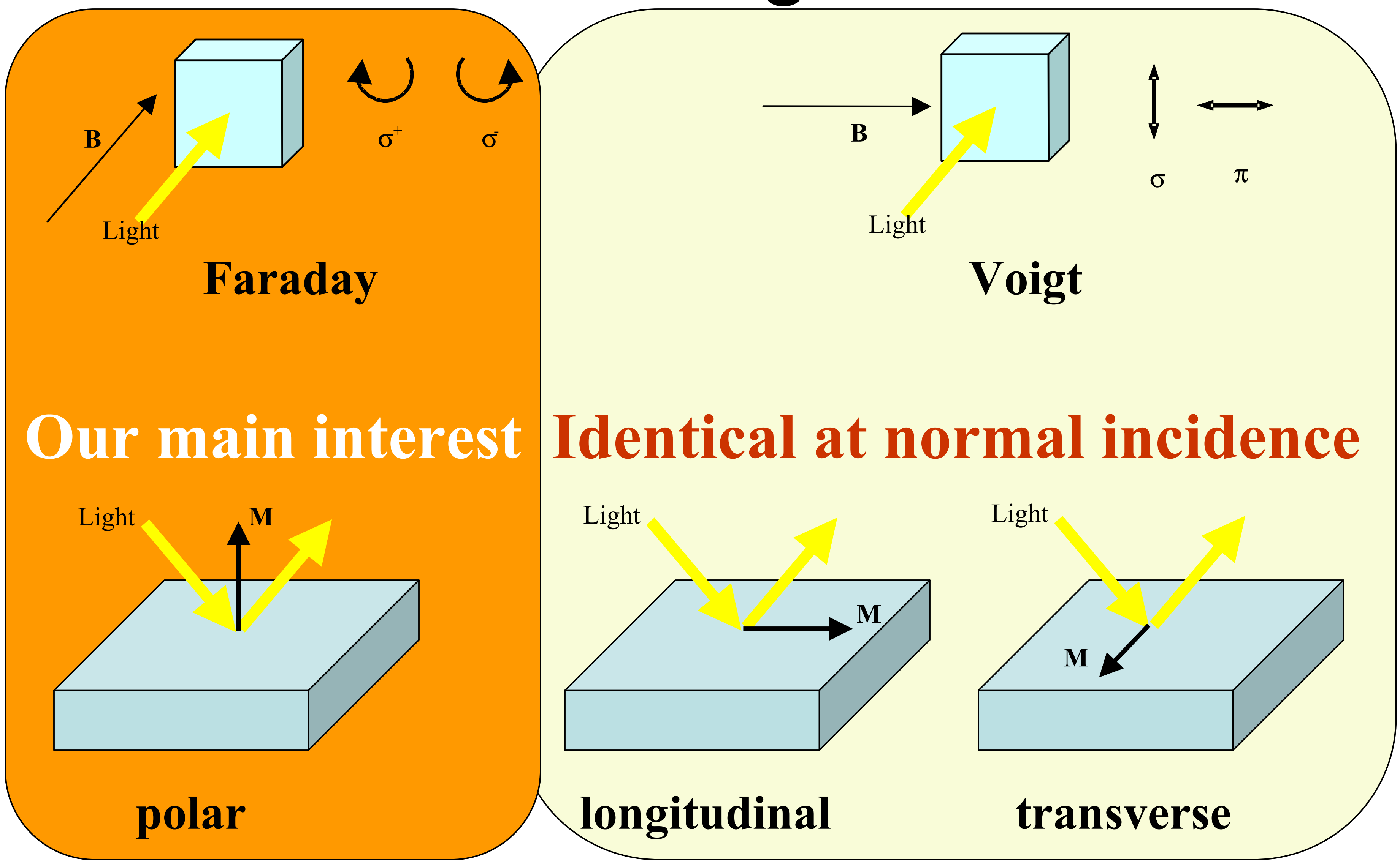

See, e.g., Chun-Yeol You and Sung-Chul Shin, Appl. Phys. Lett. **69,** 1315 (1996).

Information from interband magnetooptics

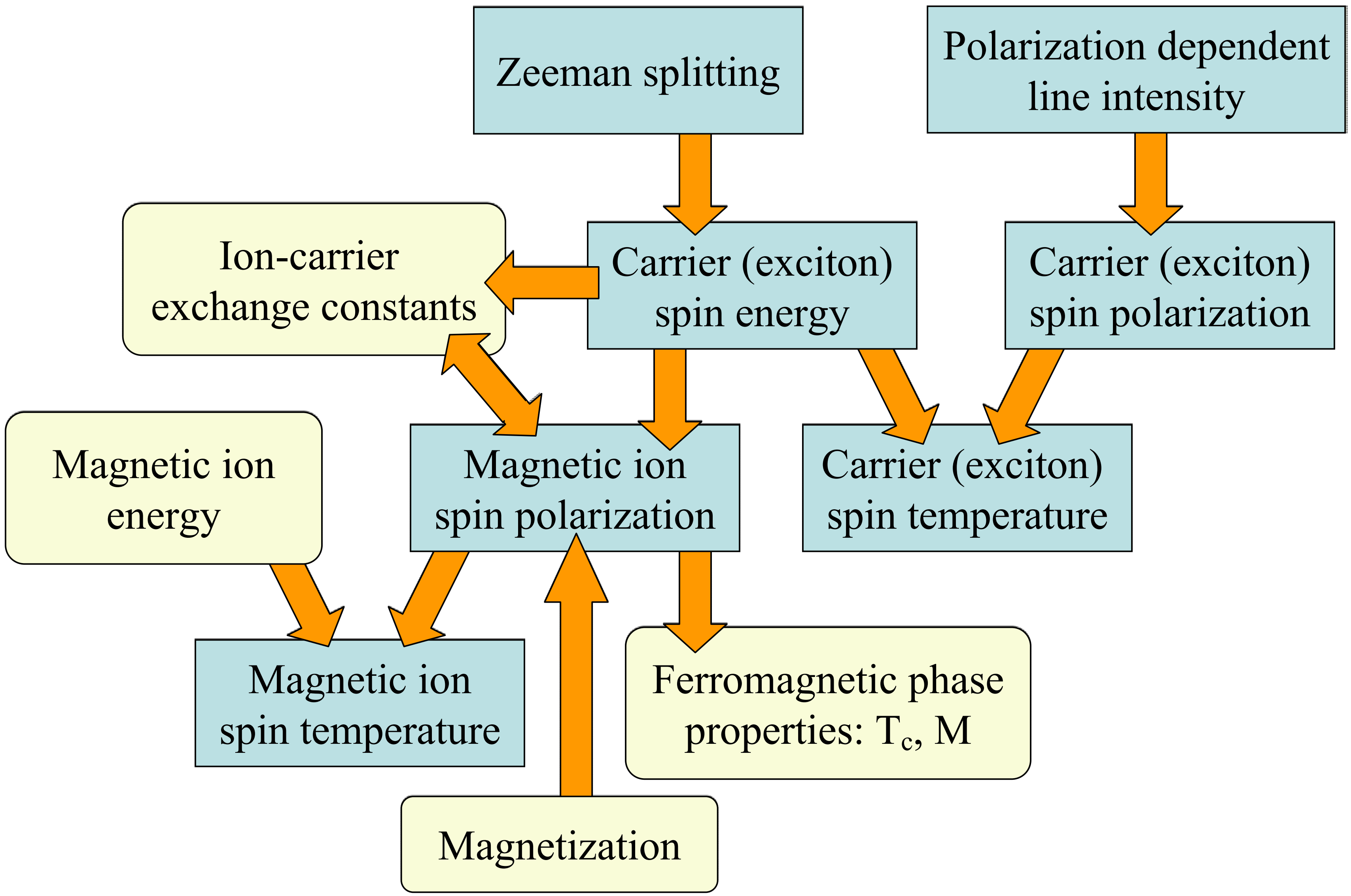

Selected examples

Looking at spins

Zeeman effect from Faraday rotation

exciton line in a (Cd,Mn)Te QW

Zeeman component predominant

Testing coherency

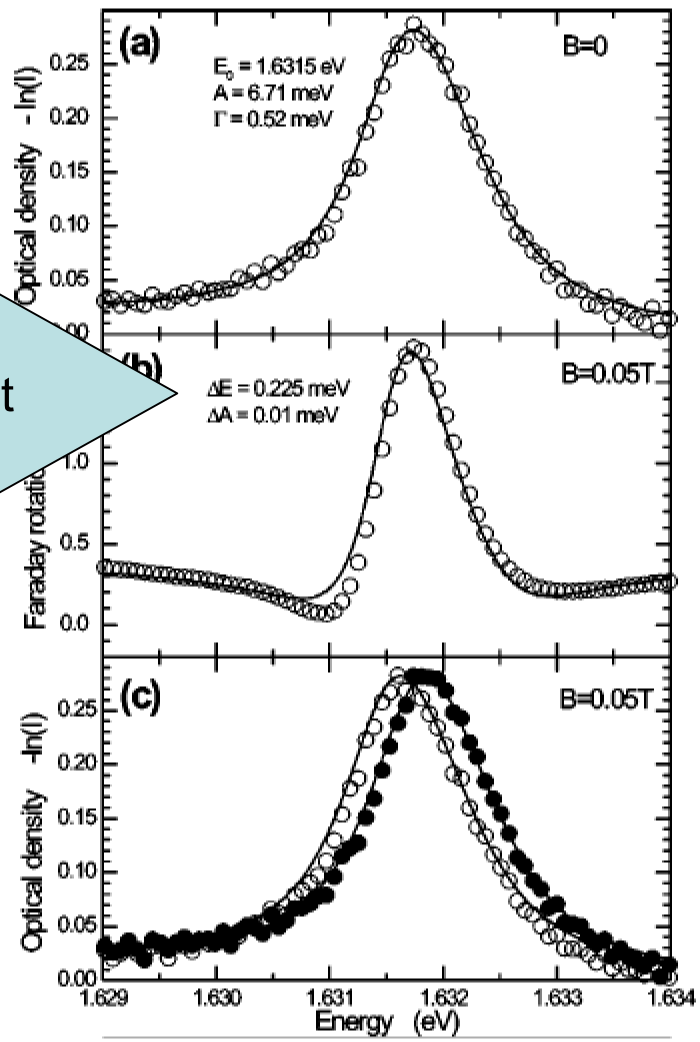

W. Maślana et al., Phys. Rev. B **63,** 165318 (2001)

Zeeman splittings of excitons in (Zn,Co)O from reflectivity

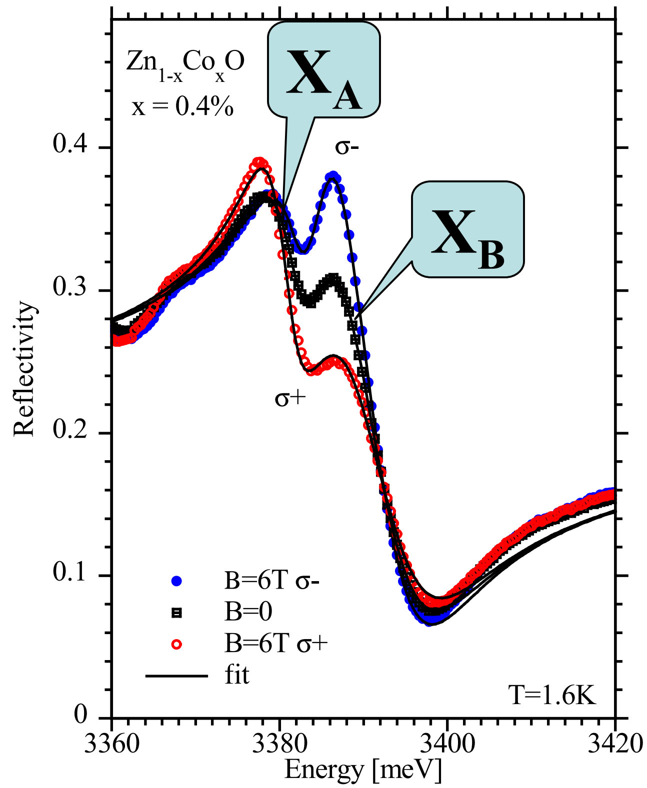

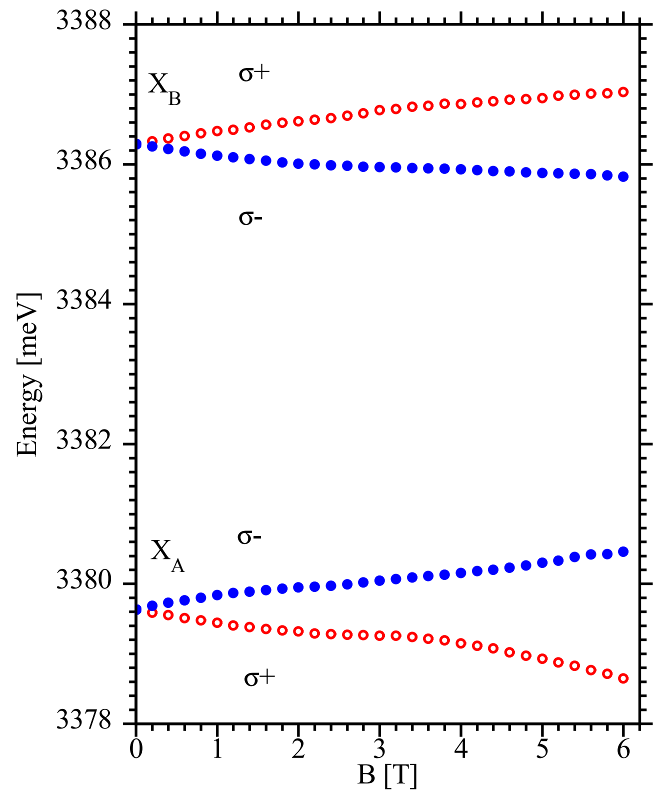

D. Ferrand et al., Journal of Superconductivity **18**, 15 (2005)

Zeeman effect of excitons in a GaN layer from Kerr rotation

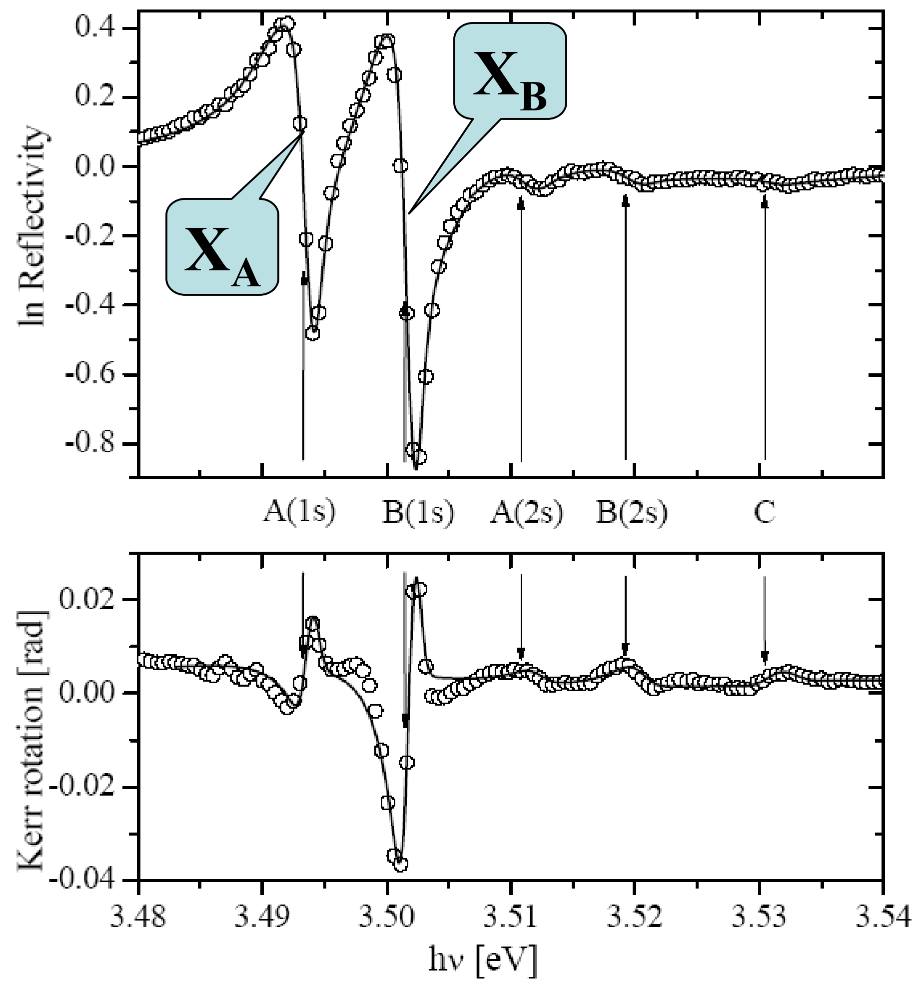

Exciton splittings at 6T
from fit of Kerr rotation

A: 0.09 meV
B: 0.16 meV

A. Golnik et al., Sol. State Commun. **124,** 89 (2002).

Spontaneous magnetization in a ferromagnetic (Cd,Mn)Te QW from zero-field PL Zeeman splitting

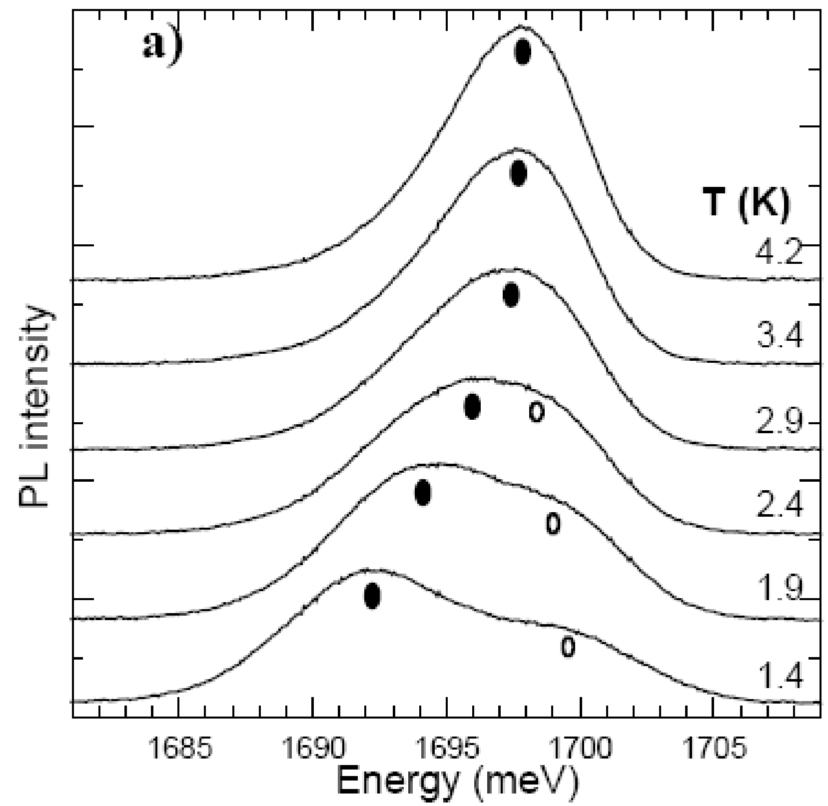

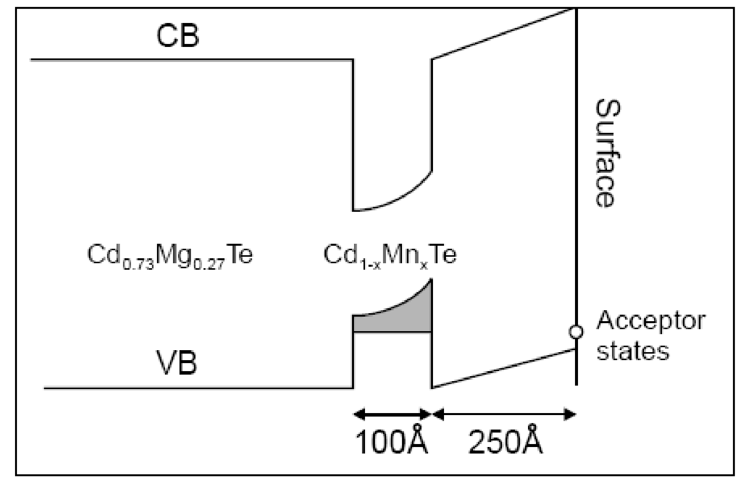

Temperature dependence of zero field PL spectra for the surface-doped sample with 4.3% Mn in QW. The hole gas density is $1.9 \times 10^{11} cm^{-2}$.

W. Maślana et al., Proc. ICPS 26 (2004)

Efficiency of electron spin injection into a GaAs QW

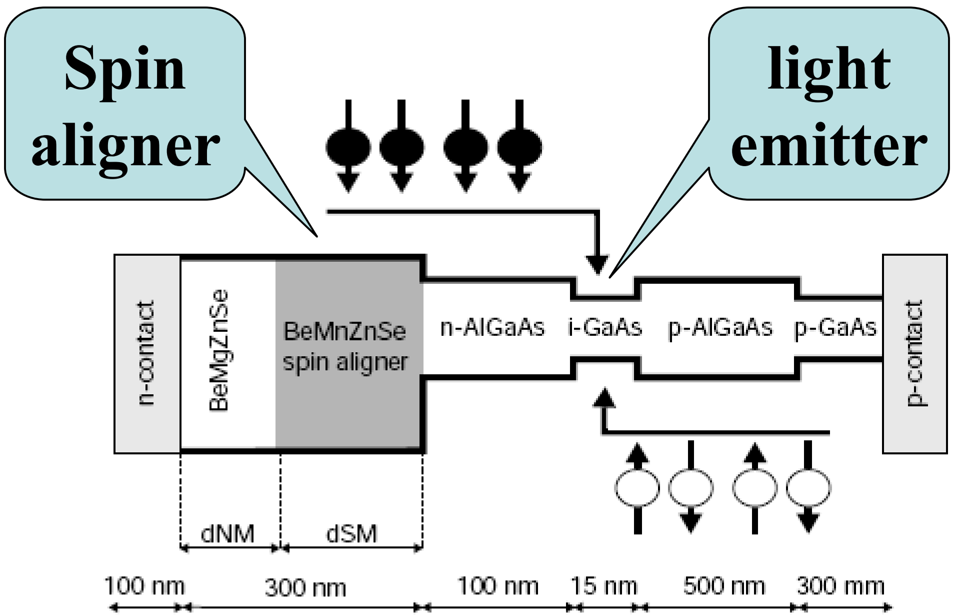

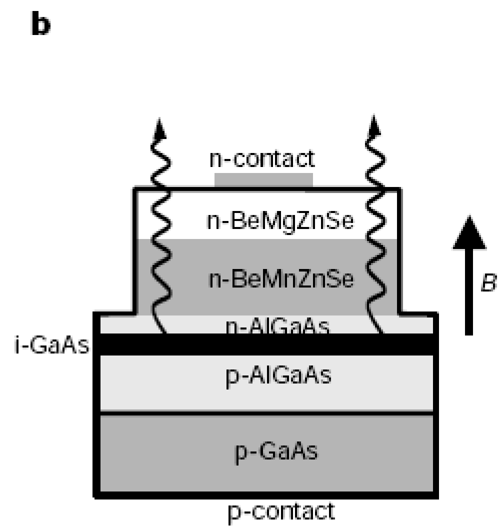

R. Fiederling et al., Nature **402**, 787 (1999)

Light → spin polarization

$$P_{opt} = \frac{I_+ - I_-}{I_+ + I_-}$$

Optimal parameters

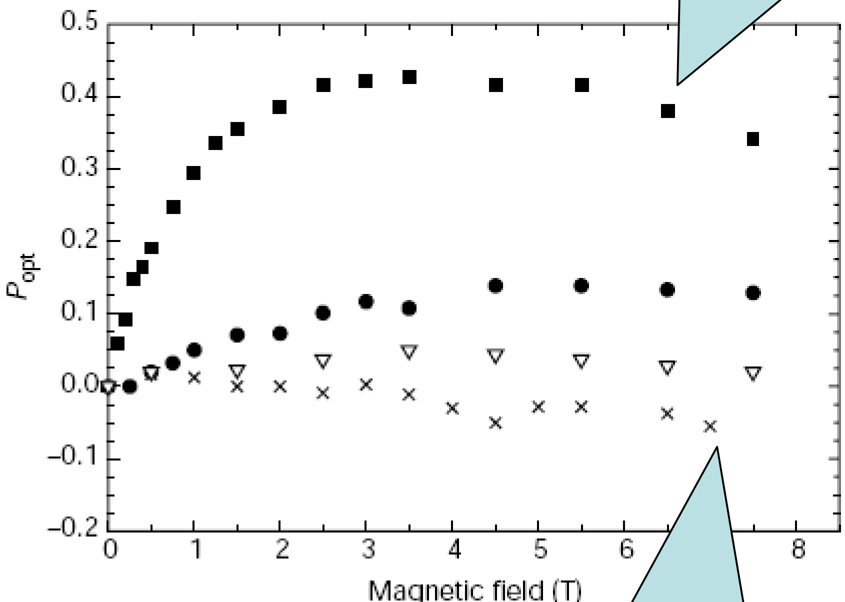

GaAs ref. layer

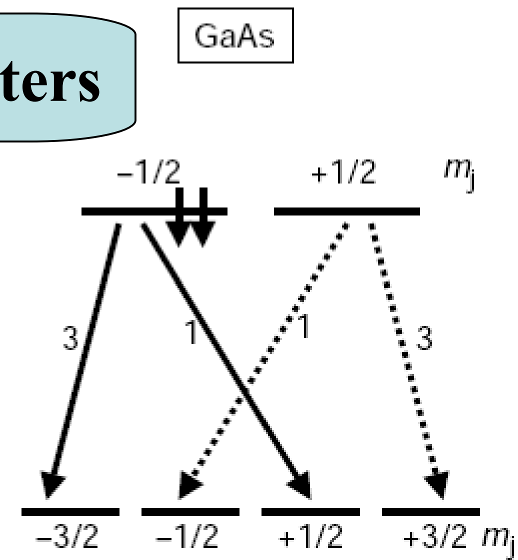

$$P_{opt} = \frac{(3n^{\uparrow} + n^{\downarrow}) - (3n^{\downarrow} + n^{\uparrow})}{(3n^{\uparrow} + n^{\downarrow}) + (3n^{\downarrow} + n^{\uparrow})}$$

3D zb case

R. Fiederling et al., Nature **402**, 787 (1999)

2D hole gas spin polarization in a (Cd,Mn)Te QW

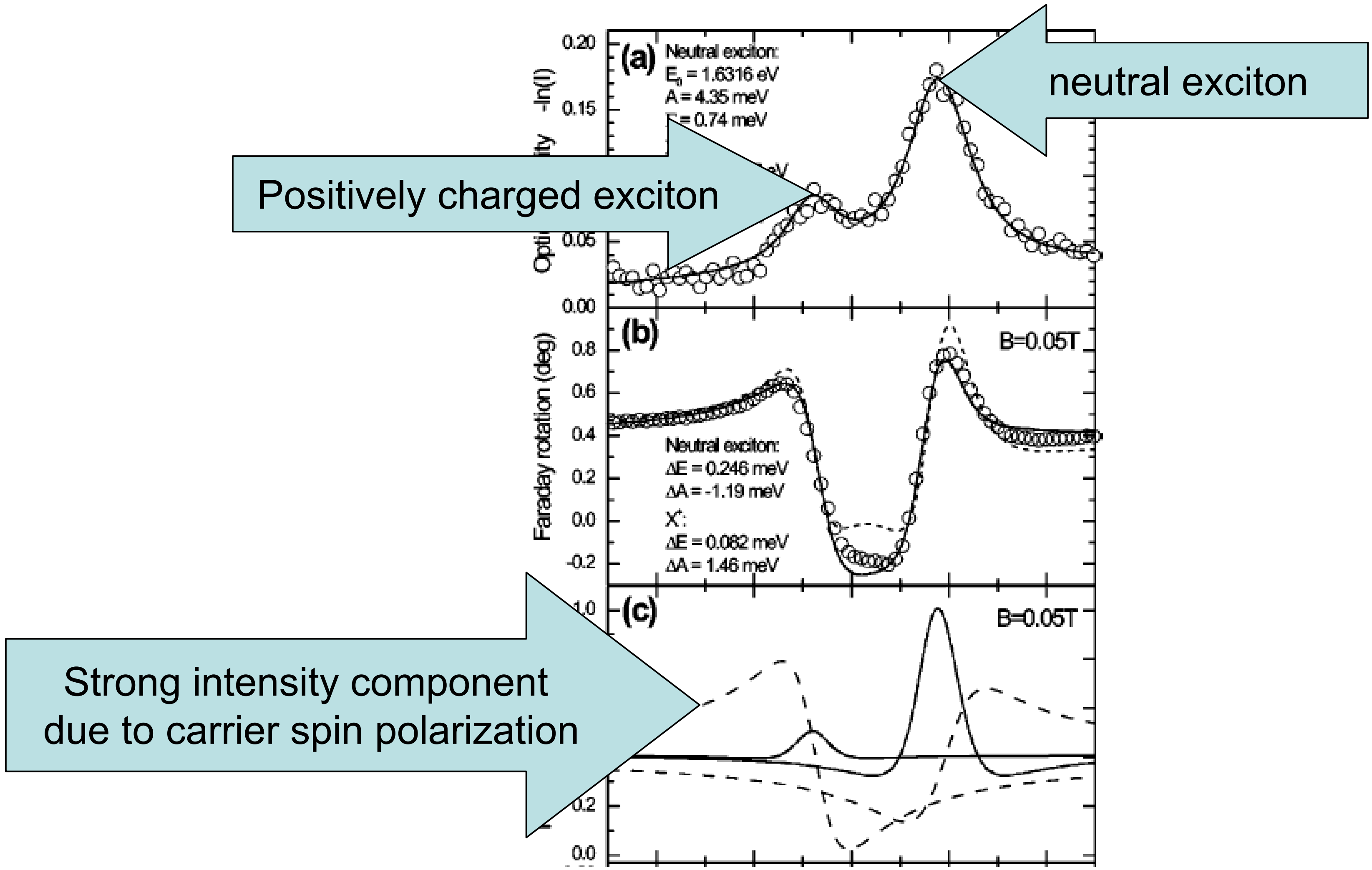

W. Maślana et al., Phys. Rev. B **63,** 165318 (2001)

Mn spin temperature in a (Cd,Mn)Te QW

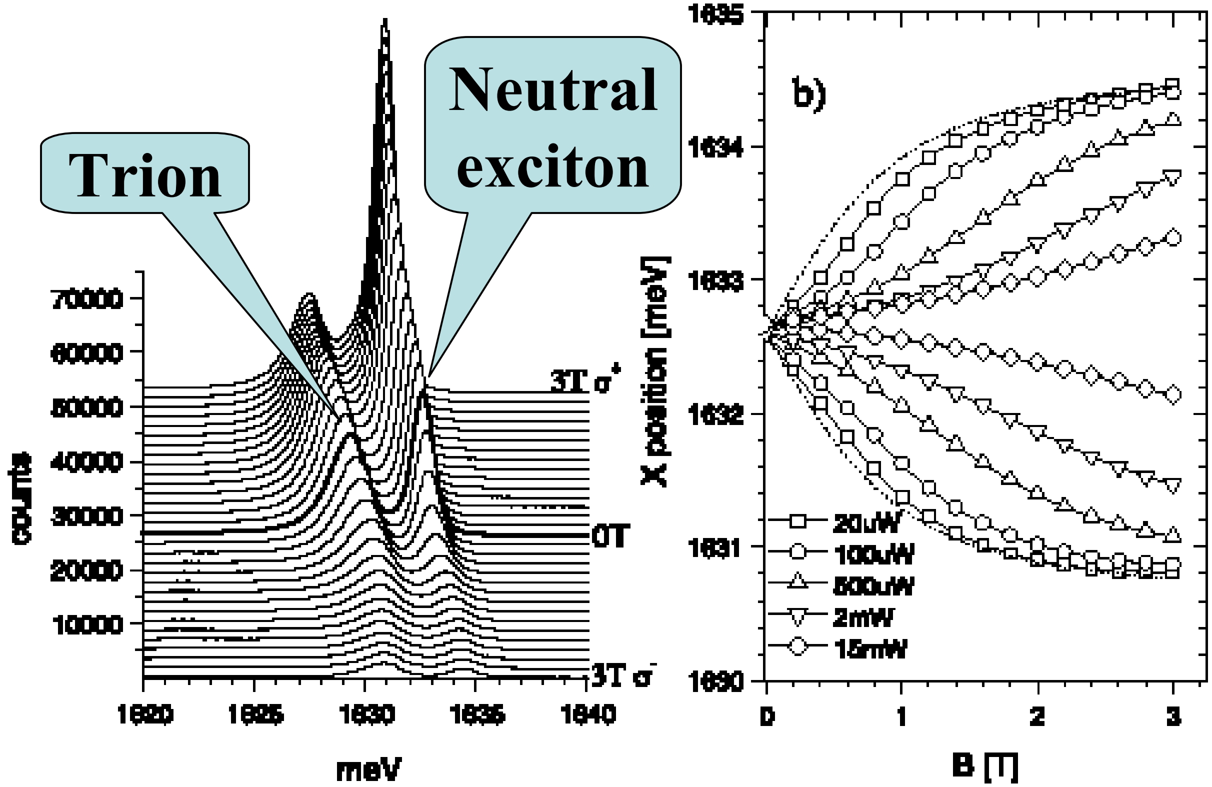

(a) photoluminescence spectra in both circular polarizations at T = 1.6 K and in magnetic field up to 3 T,
(b) neutral exciton PL peak position versus magnetic field for indicated values of excitation power.
Dotted line shows modified Brillouin function parameterization.

A. Golnik et al., Sol. State Comm. **131,** 283 (2004)

TIME-RESOLVED MAGNETO-OPTICAL KERR EFFECT (TRMOKE)

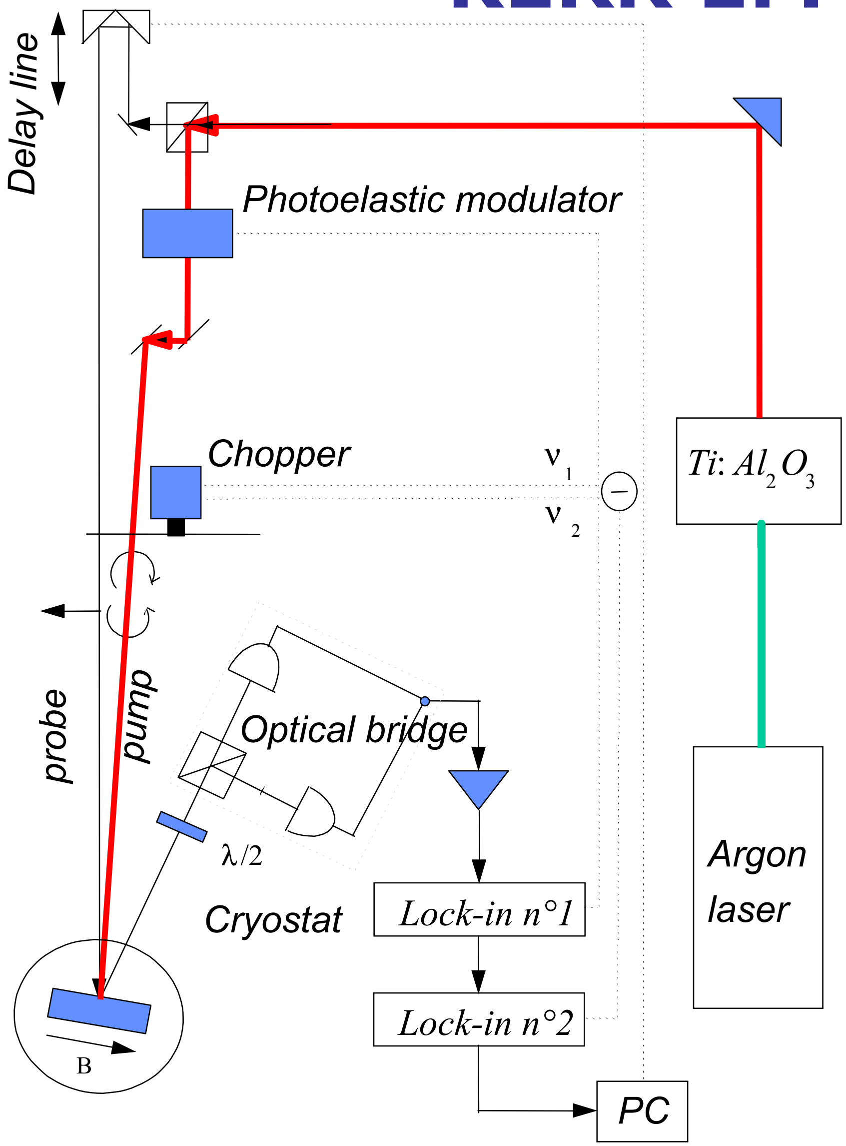

- Laser pulse: ~100 fs
- Total optical power: 3-8 mW
- Repetition rate: 82 MHz
- Magnetic field: 0 - 6T
- Temperature: 1.8-300K
- Angular resolution:1'' ($2.8*10^{-4}$ deg)
- A.Y.Elezzabi, M.R.Freeman, M.Johnson, PRL 77, 3220 (1996) (0.1 μrad)

F. Teppe et al., Sol. State Comm. **128,** 403 (2003)

2D spin imaging in n-doped CdTe

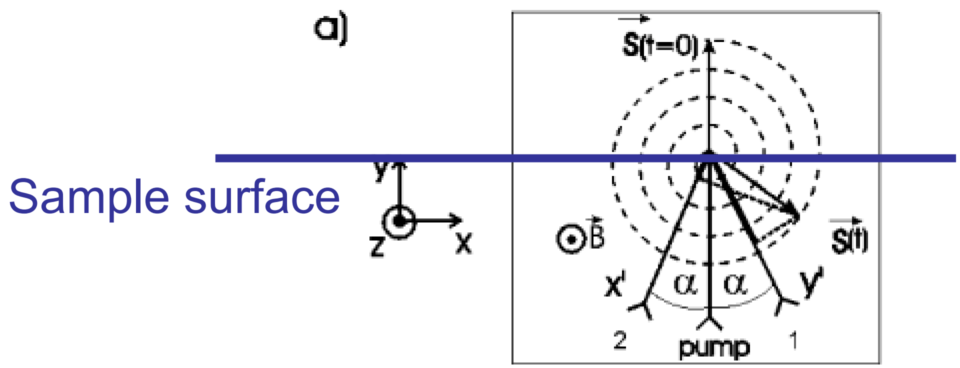

Two components of the spin vector measured through Kerr rotation along probe directions 1 and 2

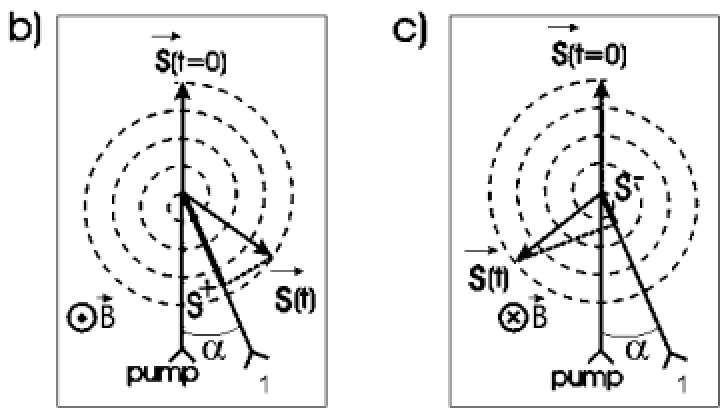

Instead of switching from direction 1 to 2, it is enough to reverse the magnetic field

F. Teppe et al., Sol. State Comm. **128,** 403 (2003)

Imaging spin precession in 2D

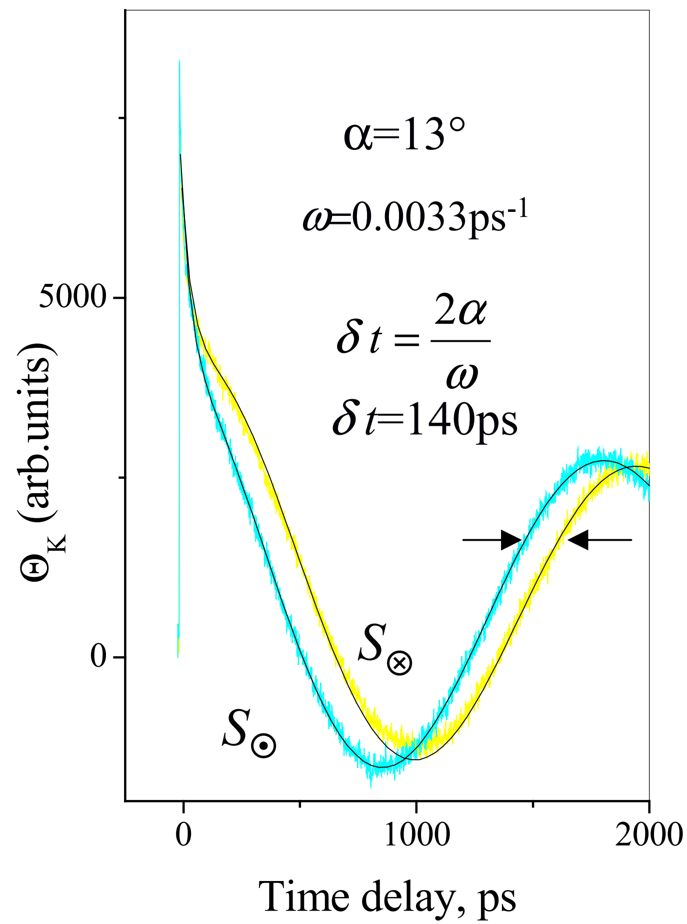

B=230G

T=2K

CdTe:Al.
$n_D=8x10^{16}$
M1371

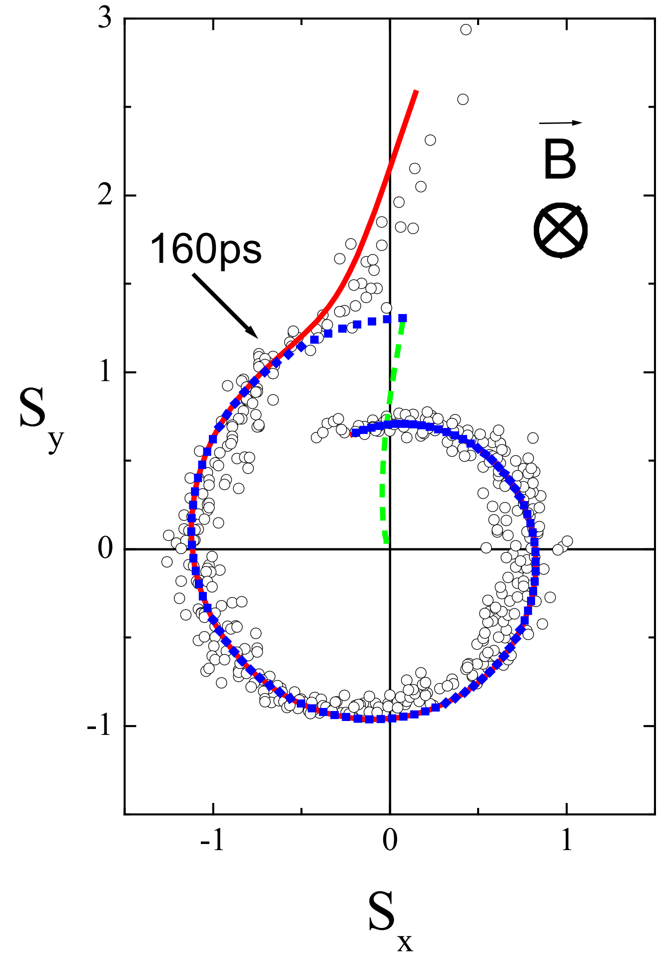

•Total spin polarization vector

•Donor-bound electron

•Free exciton

$$\Theta_K = \Theta_0 + \left(A \exp\frac{(t_0 - t)}{t_1} + B \exp\frac{(t_0 - t)}{t_2} \right) \cos(\omega(t - t_0) + \varphi)$$

F. Teppe et al., Sol. State Comm. **128,** 403 (2003)

Microphotoluminescence mapping

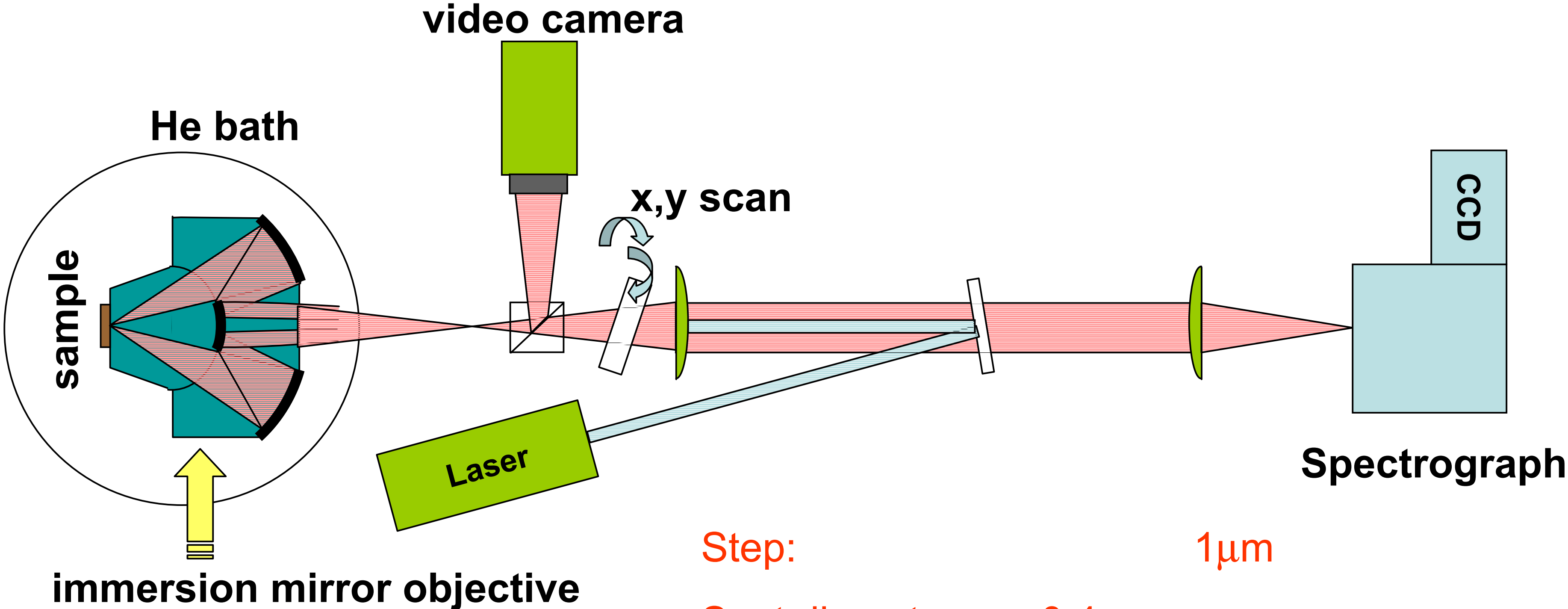

Step: 1μm

Spot diameter: 0.4μm

Area: 32μm x 32μm

Magnetic field: 0 to 5T

A. Golnik et al., Sol. State Comm. **131** 283 (2004)

Mapping of Mn spin temperature in a (Cd,Mn)Te QW

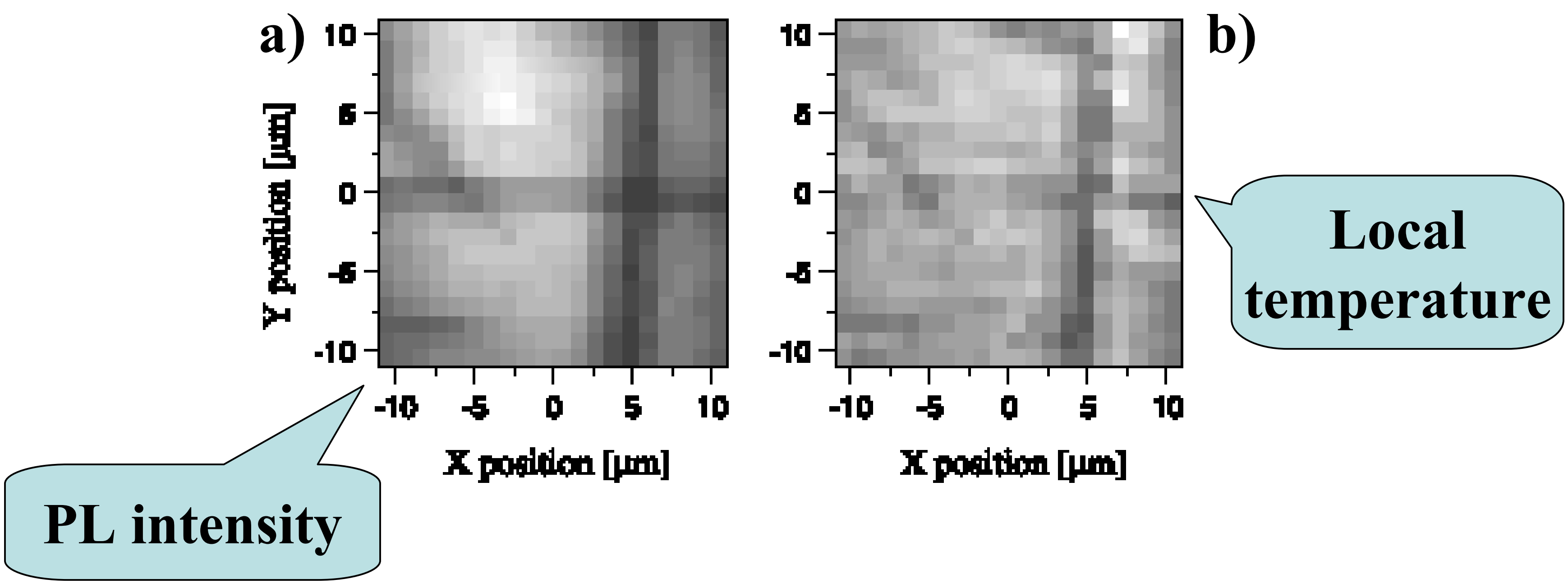

Maps of total PL intensity (a) and local temperature (b) measured with excitation photon energy 488 nm (excitation in the barrier). The helium bath temperature was 1.55 K. The scale of temperatures on (b) ranges from 1.5 K (black) to 18 K (white).

A. Golnik et al., Sol. State Comm. **131** 283 (2004)

Mapping of Mn spin temperature in a (Cd,Mn)Te QW

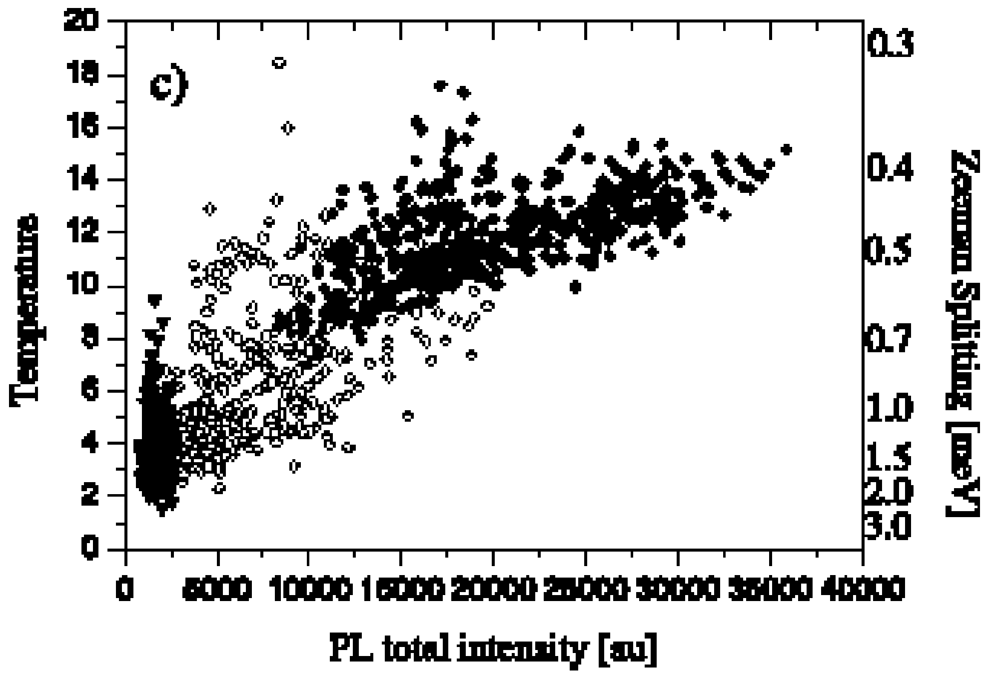

(c) Correlation of local temperature and PL intensity at different excitations: 488 nm (in the barrier) - full symbols, 680 nm (in the QW) - open symbols.

A. Golnik et al., Sol. State Comm. **131** 283 (2004)

Ferromagnetic p-doped (Cd,Mn)Te QW
determination of parameters

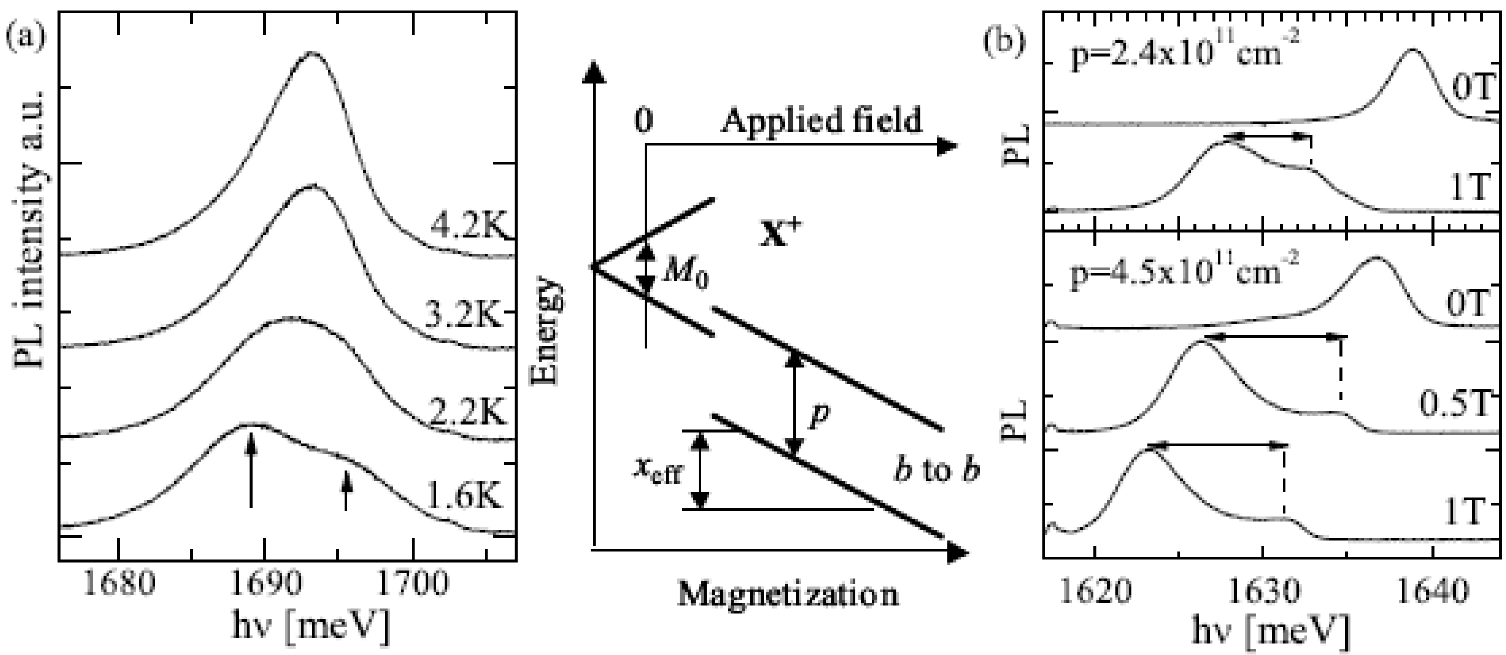

- (a) PL at zero field, from the sample with 4.65% Mn, at different temperatures. The arrows show the zero field splitting of the charged exciton (X+ in the central scheme) induced by the spontaneous magnetization M0;
- (b) PL from a QW with 1.4% Mn, at two values of the carrier density. The arrows on the double line (which is close to a band to band transition, b to b in the central scheme) indicate the splitting used to measure the carrier density.

W. Maślana et al., cond-mat/0405657 v2

Ferromagnetic p-doped (Cd,Mn)Te QW

maps of parameters

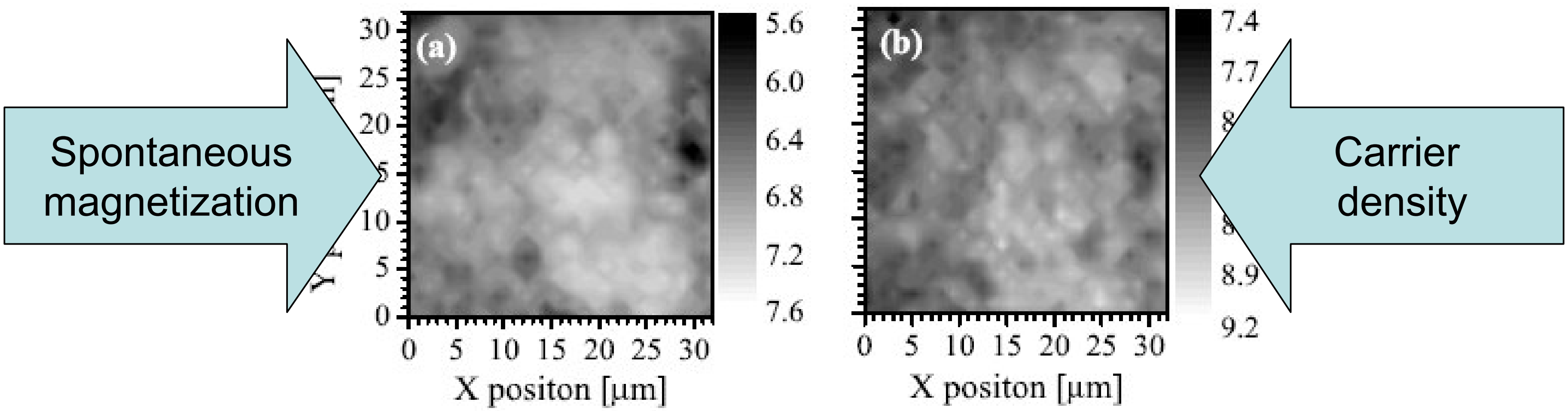

(a) zero field splitting (in meV)

(b) splitting between two components of a σ^+ PL line at B = 1 T (in meV)

W. Maślana et al., cond-mat/0405657 v2

Ferromagnetic p-doped (Cd,Mn)Te QW
correlation of parameters

no correlation with Mn concentration

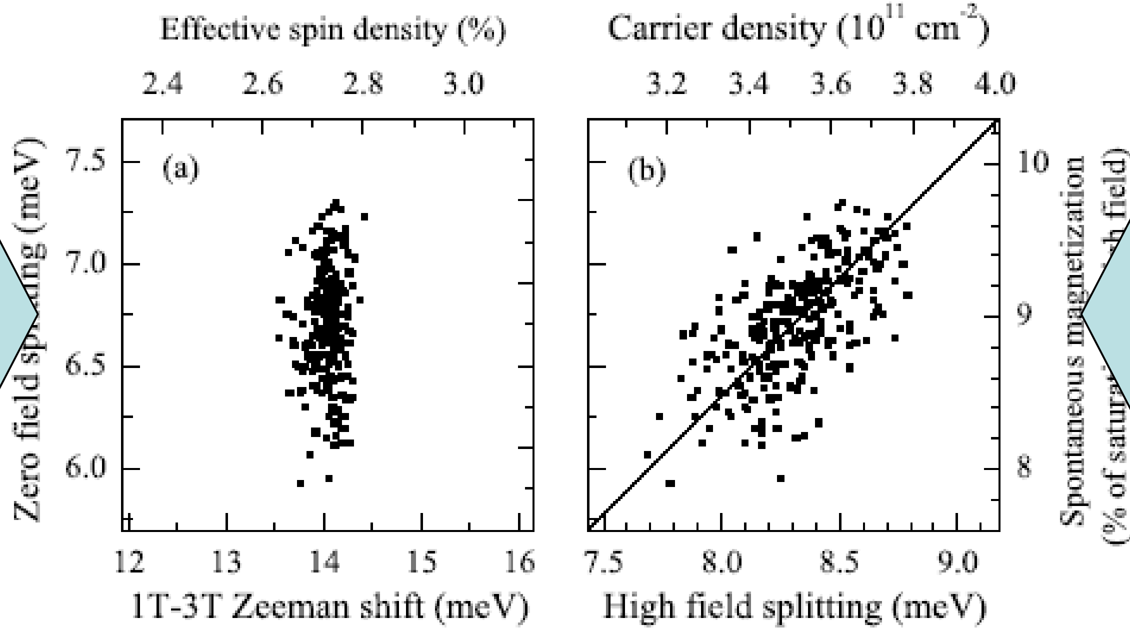

correlation with carrier density

W. Maślana et al., cond-mat/0405657 v2

Mapping of ferromagnetic domains

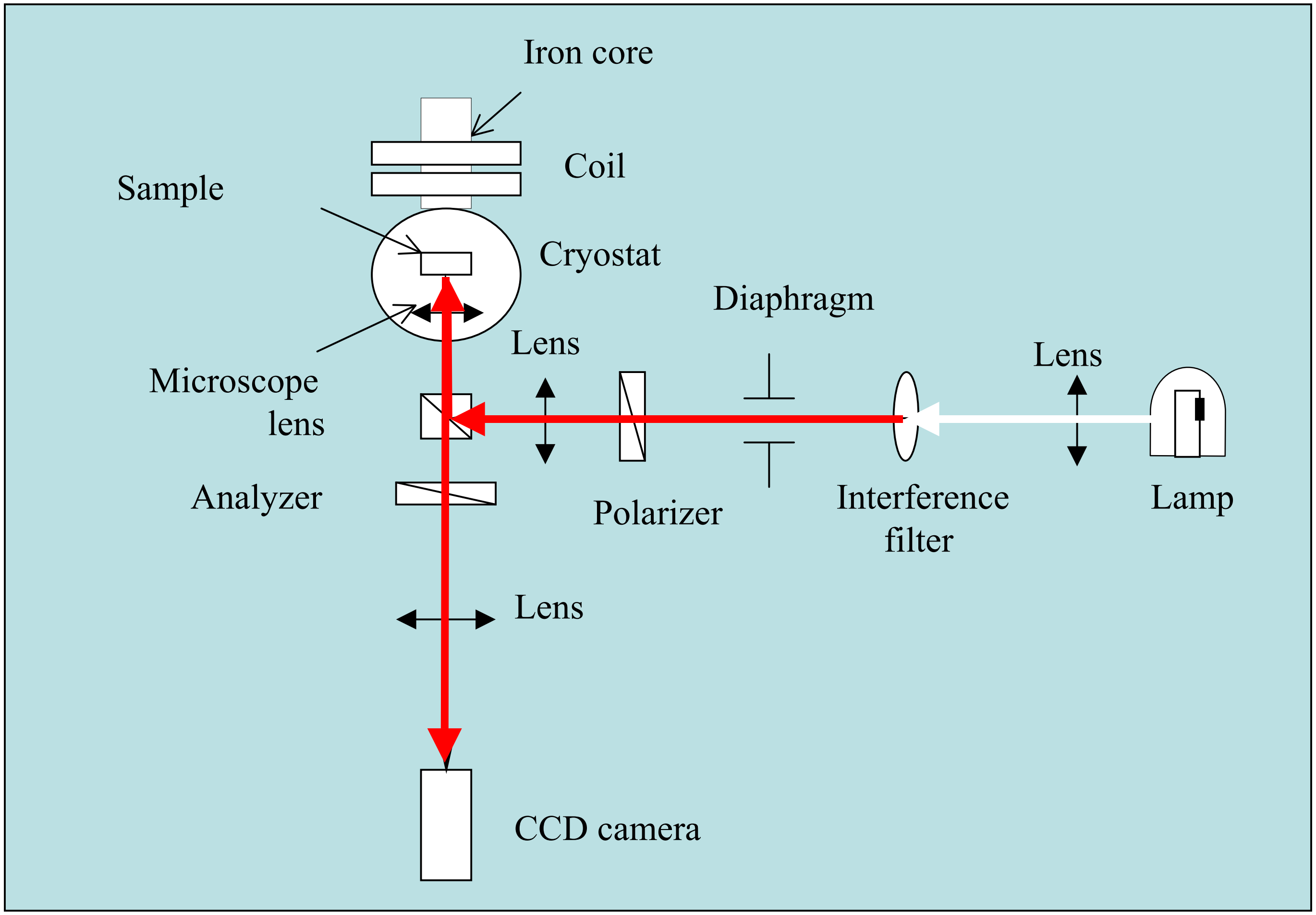

C. Gourdon INSP Paris 2005

Ferromagnetic domains in (Ga,Mn)As

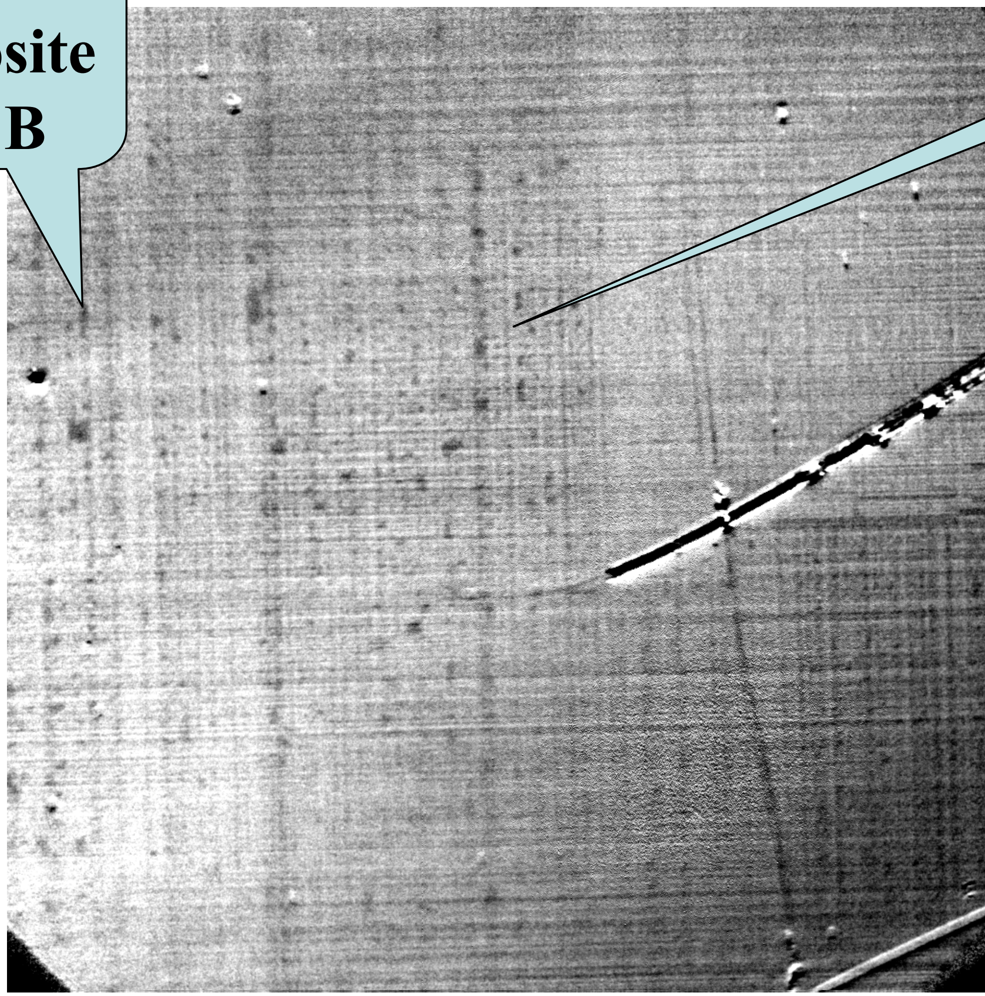

1.8 K

129 G to 156 G

$Ga_{0.95}Mn_{0.05}As$

200 nm

$\mu_0 M_s$=230G

magnetization // growth axis

C. Gourdon INSP Paris 2005

Spin flow imaging in n-GaAs

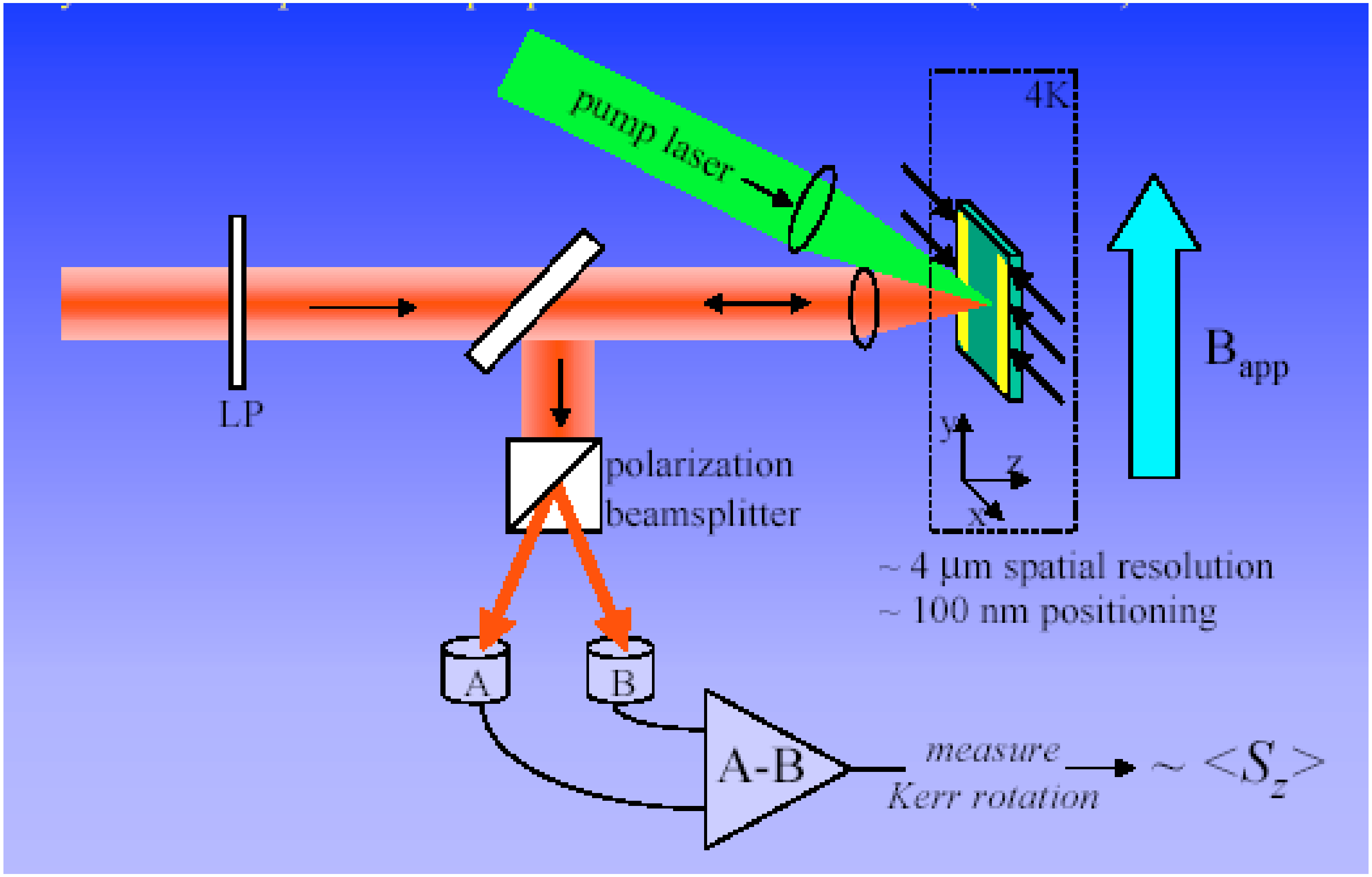

S. A. Crooker and D. L. Smith, PRL **94**, 236601 (2005)

Spin flow imaging by Kerr rotation

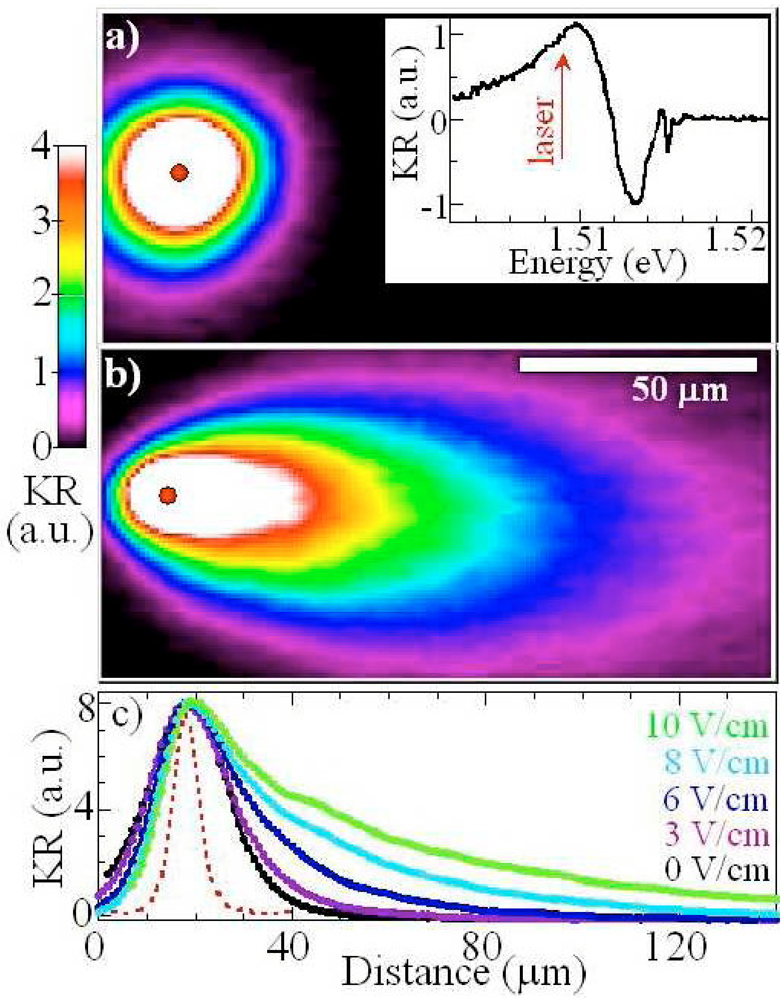

- Spin diffusion
- Spin drift and diffusion

S. A. Crooker and D. L. Smith, PRL **94**, 236601 (2005)

Uniaxial stress

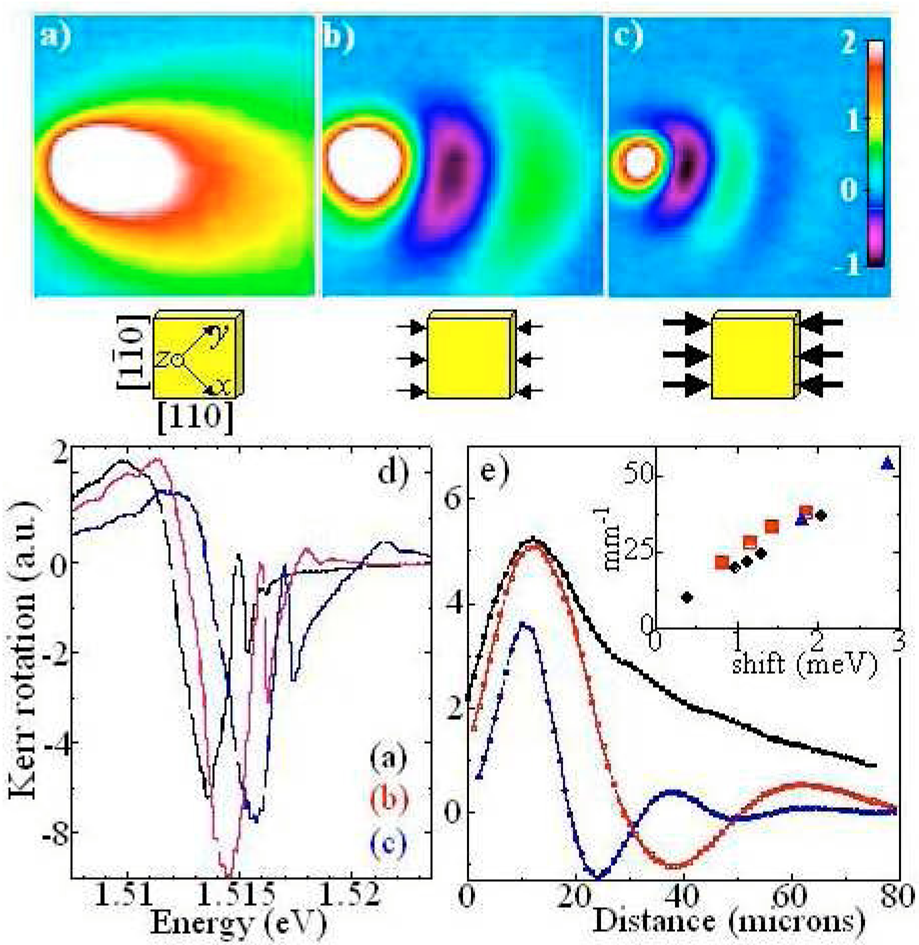

$H_S = c_3\boldsymbol{\sigma} \cdot \varphi$,
where $\varphi \propto |\mathbf{k}|$
depends on shear strain;

H_S has similar symmetry
to Rashba Hamiltonian
$H_R \propto \boldsymbol{\sigma} \cdot (\mathbf{k} \times \mathbf{E}_z)$

S. A. Crooker and D. L. Smith, PRL **94**, 236601 (2005)

Stress compared with magnetic field

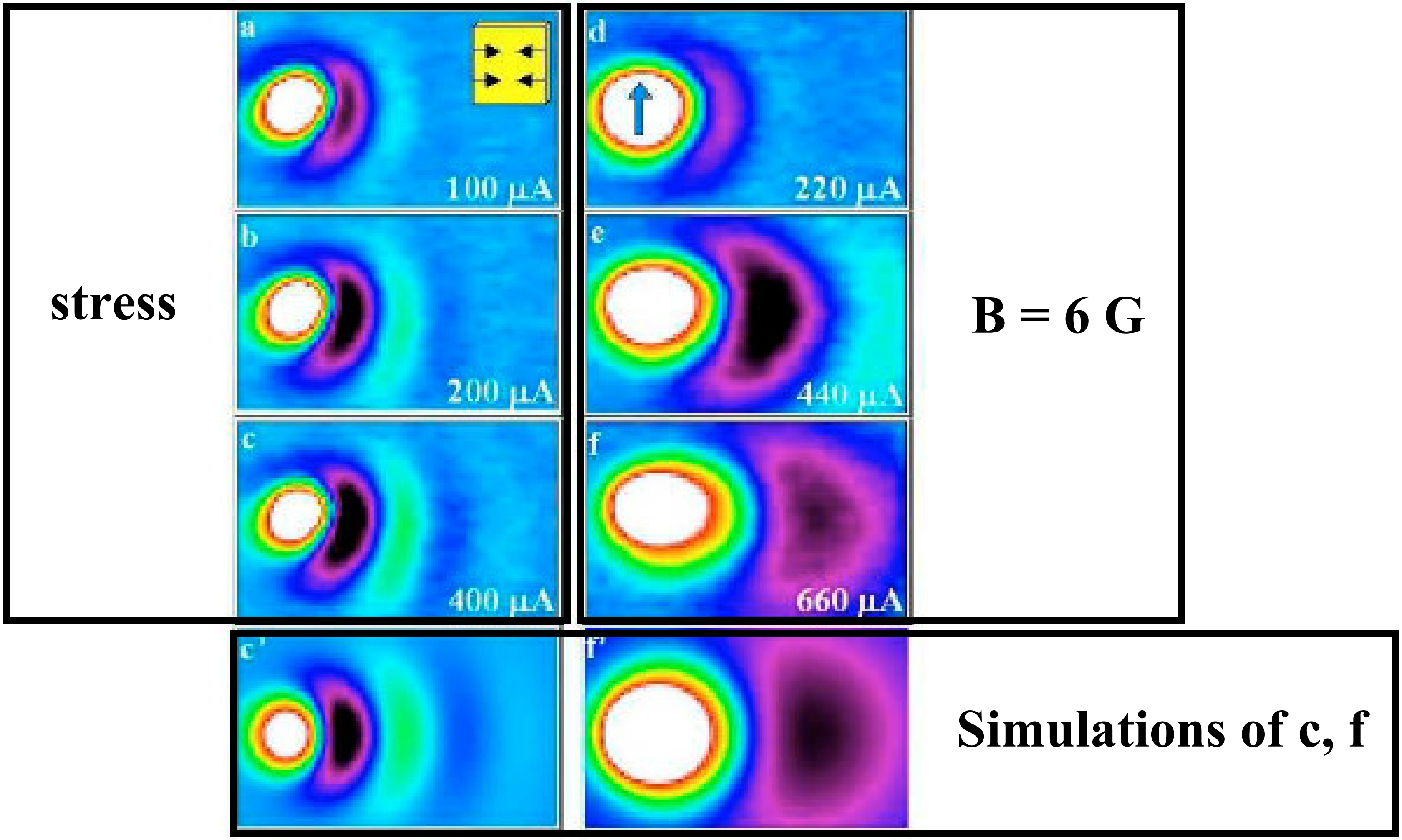

50×80 μm images of 2D spin flow at 4K with increasing |k| (current)

S. A. Crooker and D. L. Smith, PRL **94**, 236601 (2005)

Stress combined with magnetic field

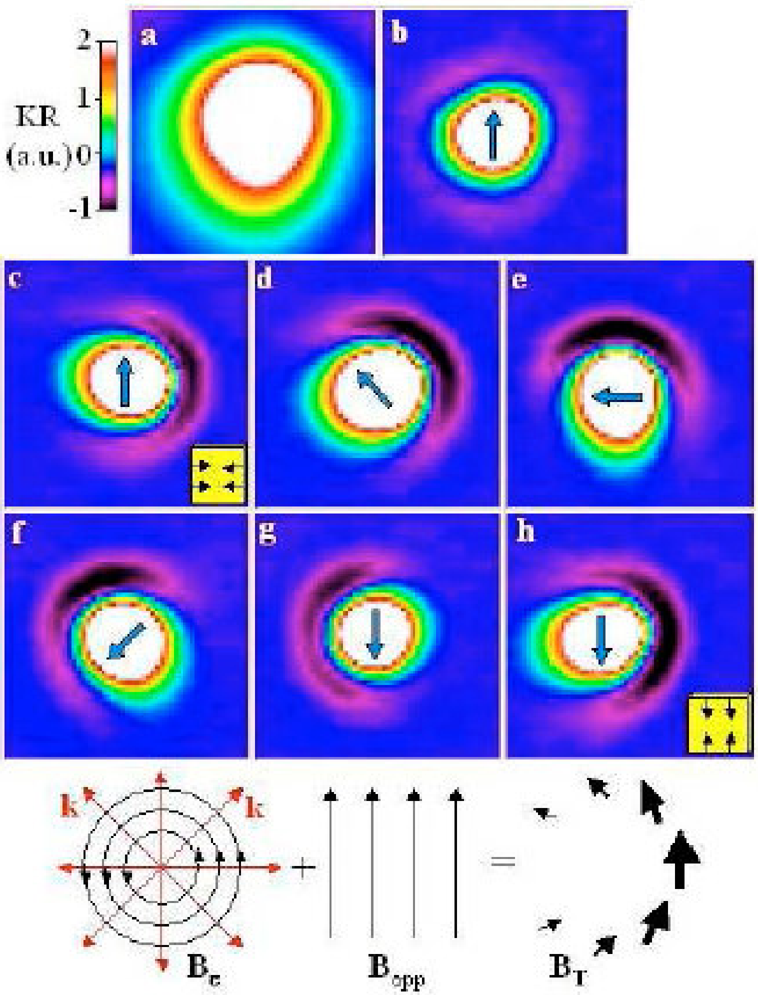

50×50 μm images of 2D spin diffusion (E=0) at 4K.

(a) Stress=0, B_{app}=0.

(b) Stress=0, B_{app}=16 G oriented along [1-10] as shown.

(c) B_{app}=16 G, with [110] uniaxial stress. Spins diffusing to the right precess, while those diffusing to the left do not. Thus B_ε is chiral for radially-diffusing electrons (see diagram).

(d-g) Maintaining [110] stress, B_{app} is rotated by 180 degrees in-plane.

(h) Stress is switched to [1-10], reversing chirality of B_ε.

S. A. Crooker and D. L. Smith, PRL **94**, 236601 (2005)

Conclusions

- Magnetooptics enables us to see spins of carriers and magnetic ions in bulk semiconductors and quantum structures
- Spin energy, polarization, temporal evolution and spatial distribution can be measured
- Parameters related to spin can be determined, such as g-factor, relaxation time, diffusion length, ion-carrier coupling constants, Curie temperature, etc.